Oxford Poverty & Human Development Initiative (OPHI)
Oxford Department of International Development
Queen Elizabeth House (QEH), University of Oxford

OPHI *RESEARCH IN PROGRESS SERIES* **58a**

On Track or Not? Projecting the Global Multidimensional Poverty Index

Sabina Alkire,[*] Ricardo Nogales,[**] Natalie Naïri Quinn,[***] and Nicolai Suppa[****]

July 2020

Abstract
In this paper we compute projections of global multidimensional poverty. We use recently published estimates of changes over time in multidimensional poverty for 75 countries, which are based on time-consistent indicators. We consider and evaluate different approaches to model the trajectories of countries' achieved and future poverty reduction. Our preferred model respects theoretical bounds, is supported by empirical evidence, and ensures consistency of our main measure with its sub-indices. We apply this approach to examine whether countries will halve their poverty between 2015 and 2030 if observed trends continue. Our results suggest that if observed trends continue, 47 countries will have halved their poverty by 2030—irrespective of the underlying model. As the current COVID-19 pandemic may severely disrupt progress in poverty reduction, we also assess its potential impact using simulation techniques and evaluate the resulting setback. Our analyses suggest a setback to multidimensional poverty reduction of about 3–10 years.

Keywords: multidimensional poverty, projection, COVID-19, poverty dynamics, SDG

JEL classification: I32, C53

Funding Information: This publication arises from research partially funded by the John Fell Oxford University Press (OUP) Research Fund, as well as ESRC-DFID ES/N01457X/1, DfID project 300706 and Sida Project 11141. The authors are grateful to all funders for their support. Suppa gratefully acknowledges funding of the European Research Council (ERC-2014-StG-637768, EQUALIZE project), the CERCA Programme (Generalitat de Catalunya), and of the Spanish Ministry of Science, Innovation and Universities Juan de la Cierva Research Grant Programs (IJCI-2017-33950).

Citation: Alkire, S., Nogales, R., Quinn, N. N., and Suppa, N. (2020). 'On Track or Not? Projecting the Global Multidimensional Poverty Index.' *OPHI Research in Progress* 58a, University of Oxford.

[*] Sabina Alkire, OPHI, Department of International Development, University of Oxford, sabina.alkire@qeh.ox.ac.uk
[**] Ricardo Nogales, OPHI, Department of International Development, University of Oxford, ricardo.nogales@qeh.ox.ac.uk
[***] Natalie Naïri Quinn, OPHI, Department of International Development, University of Oxford, natalie.quinn@qeh.ox.ac.uk
[****] Nicolai Suppa, Centre d'Estudis Demogràfics, Autonomous University of Barcelona, Spain and EQUALITAS and OPHI, nsuppa@ced.uab.es.

1 Introduction

In the report of the World Bank Commission on Monitoring Global Poverty that he chaired, Sir Tony Atkinson observed that the exercise of measuring global poverty is "highly controversial". While acknowledging that some might even regard the exercise as futile, he argued that "estimates of global poverty are flawed but not useless. By focusing on changes over time, we can learn—taking account of the potential margins of error—about the evolution of global poverty" (World Bank, 2017, p xvi). That report articulated precise yet practical strategies to address many of the fundamental issues in assessing poverty trends, where poverty is considered according to both national and international definitions and is measured in monetary and multidimensional spaces.

A more detailed account of the evolution of poverty directs attention towards the exact poverty trajectories that countries follow. Any such exercise is, however, challenged by another set of issues. In particular, for many countries, poverty estimates are only available for very few points in time. Underlying survey datasets are usually only updated every 3–5 years or even only once a decade. As a consequence, information is often not available to account for the most recent progress, nor to determine the extent to which it could be affected by external shocks.

These issues also cause challenges for obtaining global aggregates where, moreover, country estimates are observed in different years and with different periodicities. Thus, it is not obvious how to aggregate achieved trends across countries in a coherent and rigorous way. Likewise, little can be said about the recent levels of poverty at the global level. Methods have been developed for predicting global monetary poverty aggregates, and underlie claims such as that in 2015 more than a billion fewer people globally were living in extreme monetary poverty than in 1990 (World Bank (2018) cf. Ravallion (2013)). While sharing several data limitations, analogous multidimensional poverty analyses entail additional methodological challenges. This may partly explain why projections of multidimensional poverty are still rare in the literature; to our knowledge, Ram (2020) is the first such study. There has therefore been no basis to assess the impacts of exogenous shocks on such trends. To close this gap is the aim of our paper.

We draw upon the just-released study of harmonized trends in the global Multidimensional Poverty Index (MPI), which covers 75 countries with a combined population of about five billion people at two points in time (Alkire *et al.*, 2020c,d).[1] The global MPI as proposed in Alkire and Santos (2014) uses the method proposed by Alkire and Foster (2011) and

[1] Alkire *et al.* (2020c,d) update and extend Alkire *et al.* (2017), which covered 34 countries using earlier datasets. Burchi *et al.* (2020) is another recent study that computes trends in multidimensional poverty, measured with a different index, across 55 countries using the International Income Distribution Database.

is widely recognized as an internationally comparable multidimensional poverty measure. Alkire *et al.* report extensive progress in global poverty reduction. During the measured periods, 65 out of the 75 countries made significant progress in reducing multidimensional poverty, while over 50 reduced the number of people in poverty. Yet the trends story is incomplete: the time periods covered range from three to twelve years; the years span 2000–2019, with the starting year of some countries well after the ending point for others. While informative, related analyses are limited to annualized absolute or relative rates of change during the measured period, from which it is not possible to summarise aggregate trends.

To address these methodological challenges, we develop a modelling framework to compute projections of global multidimensional poverty. We use these projections in two ways. First, we seek to answer a question inspired by SDG 1 target 1.2: which countries are on track to halve multidimensional poverty between 2015 and 2030? Second, recognising that the COVID-19 pandemic that has taken hold in early 2020 has jeopardised progress, we also ask what are the plausible impacts of the pandemic on recent progress in poverty reduction in the developing world?

In seeking to make poverty projections, our work relates to similar exercises that have been conducted with other development indicators, in particular the World Bank (2018) on extreme income poverty, the work of the UN Inter-agency Group for Child Mortality Estimation (UN IGME, 2019), the monitoring of child malnutrition by WHO-UNICEF (2017), and the analysis of child mortality and education indicators by, e.g., Klasen and Lange (2012). While we build on this earlier work, none of these approaches is immediately applicable to our context.

To develop the modelling framework for our study, we consider and evaluate different approaches to model country-specific trajectories of achieved and future poverty reduction; these include linear, exponential (or constant rate of change), and logistic models. To identify the most appropriate models, we seek to respect the theoretical bounds of our poverty measures, consistency given the relationships among them, and the available empirical evidence. Specifically, we make the case for a logistic model as the most appropriate for the incidence of poverty, an appropriately modified logistic model for its intensity, and their product for multidimensional poverty itself.

Among our most salient results, we find that if observed trends continue, 47 out of 75 countries will halve multidimensional poverty between 2015 and 2030—irrespective of the underlying model. However, 18 countries are off track according to all models, while for 10 countries results are model-dependent. These results are stress-tested in counterfactual analyses, in which implied trajectories under alternative model parameters are examined. We find, for instance, that 15 countries that are off track to meet the poverty target

according to our preferred model could halve poverty by 2030 if their performance in poverty reduction were boosted to that of the median performing country. We also find that some countries that are on track to meet the poverty target may falter if their observed performance in terms of poverty reduction slows down.

As the current COVID-19 pandemic threatens to severely disrupt progress in poverty reduction, we also assess the expected increase in poverty using simulation techniques and evaluate the resulting setback. We expect substantial impacts on multidimensional poverty through two indicators which are being severely affected by the pandemic—nutrition and children's school attendance. We explore several scenarios that are informed by studies of the impact of COVID-19 conducted by international agencies, in particular UNESCO (2020) on school closures and WFP (2020) on food insecurity. Our analyses suggest a setback to aggregate poverty reduction across the 70 included countries by about 3–10 years depending on the underlying scenario.

The paper proceeds as follows. In section 2, we describe the data used in the study. In section 3, we briefly discuss approaches in the related literature, identifying those that are feasible to explore and build on in our study context. In section 4, we explore alternative models for country-level multidimensional poverty dynamics, identifying logistic trajectories as our preferred model on the basis of both theoretical adequacy and compelling cross-country evidence. In section 5, we implement these models to nowcast and to forecast multidimensional poverty, and to discuss counterfactual trajectories as stress-tests of predicted trends. In section 6, we assess the potential impact of the COVID-19 pandemic on multidimensional poverty in 2020, through simulations of scenarios based on deprivation increases predicted by UN agencies. Section 7 presents some concluding remarks.

2 Data

The primary data source for this study is the Changes over Time dataset constructed by Alkire *et al.* (2020c), which contains harmonized estimates of aggregate measures of multidimensional poverty for 80 countries in the developing world based on the structure of the global MPI. Of those, results reported in this paper focus on the 75 countries that are jointly analysed by OPHI and UNDP's Human Development Report Office (UNDP, OPHI, 2020).[2]

[2]To align with the OPHI-UNDP collaboration, results reported in this study omit five countries that a) dropped a health or education indicator in the harmonisation process, and b) experienced large absolute or relative changes in the harmonised MPI value in comparison with the non-harmonised value. The omitted countries are Afghanistan, Montenegro, Trinidad & Tobago, Viet Nam, and Yemen.

Table 1: Global MPI

Dimension of Poverty	Indicator	Deprived if ...	SDG area	Weight
Health	Nutrition	Any person under 70 years of age for whom there is nutritional information is *undernourished*.	SDG 2	$\frac{1}{6}$
	Child mortality	A child *under 18* has *died* in the household in the five-year period preceding the survey.	SDG 3	$\frac{1}{6}$
Education	Years of schooling	*No* eligible household member has completed *six years* of *schooling*.	SDG 4	$\frac{1}{6}$
	School attendance	Any school-aged child is *not attending* school *up to* the age at which he/she would complete *class 8*.	SDG 4	$\frac{1}{6}$
Living Standards	Cooking fuel	A household cooks using *solid fuel*, such as dung, agricultural crop, shrubs, wood, charcoal or coal.	SDG 7	$\frac{1}{18}$
	Sanitation	The household has *unimproved* or *no* sanitation *facility* or it is improved but *shared* with other households.	SDG 6	$\frac{1}{18}$
	Drinking water	The household's source of *drinking water* is *not safe* or safe drinking water is a *30-minute walk* or *longer walk* from home, roundtrip.	SDG 6	$\frac{1}{18}$
	Electricity	The household has *no electricity*.	SDG 7	$\frac{1}{18}$
	Housing	The household has *inadequate* housing materials in *any* of the three components: *floor*, *roof*, or *walls*.	SDG 11	$\frac{1}{18}$
	Assets	The household does *not own more than one* of these *assets*: radio, TV, telephone, computer, animal cart, bicycle, motorbike, or refrigerator, and does not own a car or truck.	SDG 1	$\frac{1}{18}$

Notes: This is a simplified version, for more details on global MPI and Changes over Time data, see UNDP, OPHI (2020) and Alkire *et al.* (2020d), respectively.

First published in the 2010 UNDP Human Development Report, the global MPI is a poverty index that is based on the joint distribution of 10 indicators, which are grouped under the dimensions of Health, Education and Living Standards (Alkire and Santos, 2014). The definitions of these indicators were revised in 2018 to better align to the SDGs (Alkire *et al.*, 2020a; Alkire and Kanagaratnam, forthcoming). Table 1 shows the current structure of the global MPI, which is the basis of all the information contained in the Changes over Time dataset, our main data for projections of multidimensional poverty. This structure also underpins the 2020 release of the global MPI (Alkire *et al.*, 2020b), whose underlying micro datasets are used for our COVID-19 impact simulations in section 6. In the global MPI structure, each dimension is assigned an equal weight (1/3), and indicators are also assigned equal weights within dimensions. A person is identified as being multidimensionally poor if they simultaneously suffer 33% of the weighted deprivations or more.

In order to ensure inter-temporal comparability for each country, the harmonisation process means that, for some of them, the Changes over Time estimates rely on slightly different indicator definitions and datasets from the 2020 global MPI. For 62 out of the 75 considered countries, the underlying microdatasets are identical in both Changes over Time and 2020 global MPI data, and for 29 countries the MPI estimates are identical (see Alkire *et al.*, 2020c,d, for more details).

Two observations are available for each country in the Changes over Time dataset. The timing of these observations depends on survey availability; the earlier observations are

dated between 2000 and 2014 (median 2010) while the later observations are dated between 2008 and 2019 (median 2014). The elapsed time between observations is between 3 and 12 years (median 5 years). The distribution of survey dates is illustrated in Figure 1, where one can see that for most countries, including Ethiopia and Sierra Leone, the difference between the observed poverty levels is between 3 to 6 years, and in many cases, both surveys are at least as recent as 2010. For some other countries, such as India and Madagascar, the available data is slightly older (2008 and 2006, respectively) and the observed poverty levels cover a 9-year time span or more. In fewer cases, we can only on data prior to 2005 for the first observed poverty level, such as in Mozambique and Bolivia. For a complete list of countries, datasets, and years of the surveys, see Table A.1 of the appendix.

Figure 1: Survey Dates

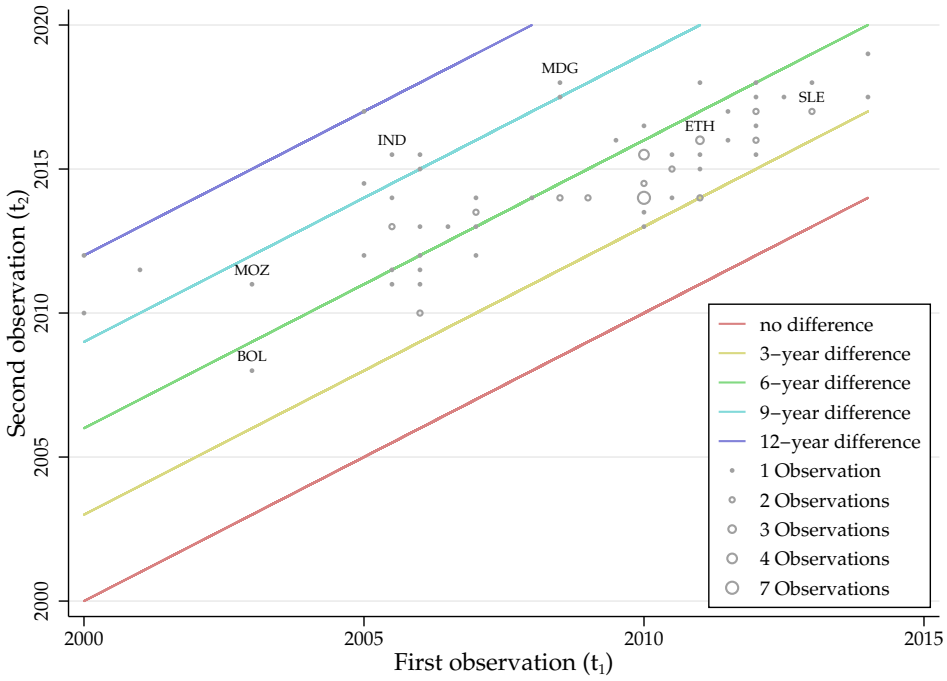

Notes: Only a few selected observations are labelled for reasons readability.

Figure 2 provides a first view of the Changes over Time data. Each dot represents the observed MPI value for a specific country at a specific point in time, and they are connected by a line when they correspond to the same country. Several insights emerge at first glance. There is considerable heterogeneity in terms of the first and second observed MPI values for each country, as well as in terms of the elapsed time span between observations. Most countries experience poverty reductions in the observed period, albeit to varying extents and with some visible exceptions, such as Benin or Serbia, where poverty has increased. Also, note that in some cases, changes in multidimensional poverty over time are minimal, such as in Benin and Serbia, and also Cameroon, Togo, Chad and Niger, among others. Finally, some countries achieved substantial poverty reduction in absolute

Figure 2: Changes over time data: The adjusted headcount ratio (MPI)

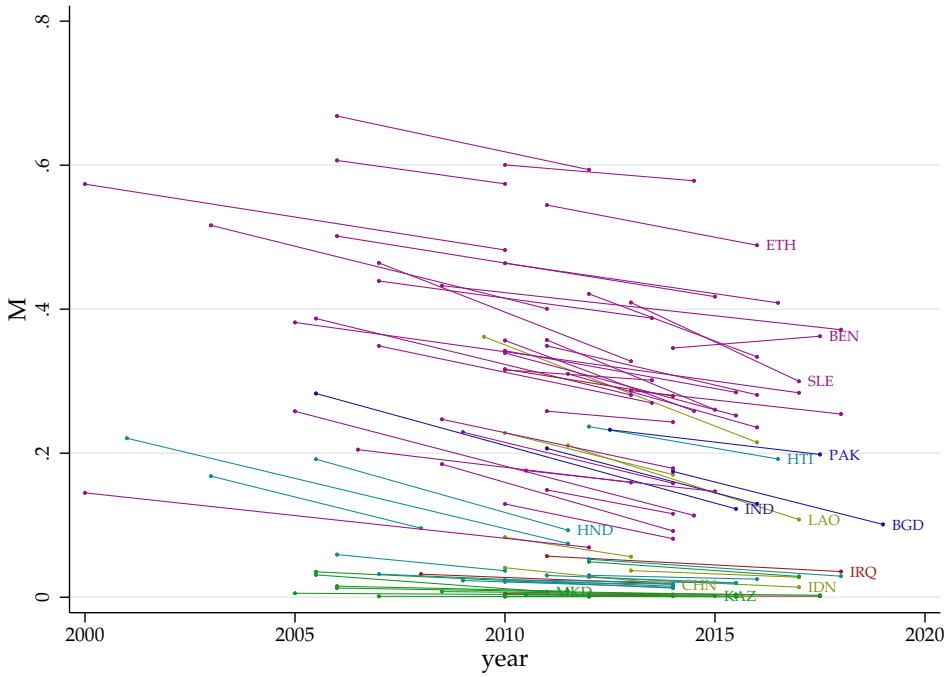

Notes: Dots represent point estimates based on micro data; Countries are colour-coded by world region: ● Arab States; ● East Asia and the Pacific; ● Europe and Central Asia; ● Latin America and the Caribbean; ● South Asia; ● Sub-Saharan Africa.

terms, for example Sierra Leone and India. For a more detailed analysis of these data see also Alkire *et al.* (2020d).

3 Projection Approaches for Development Indicators

In this study we aim to establish a modelling approach for projections of multidimensional poverty that respects theoretical requirements, which are in part specific to our measure. It must also be feasible to implement with the available data, and rest on sound empirical evidence. In this section we review the methods and applications used in similar exercises for other development indicators, as well as an earlier approach for multidimensional poverty. We assess the extent to which we may be able to adopt earlier approaches and identify where we will need to build on them.

The World Bank publishes nowcasts and forecasts of extreme monetary poverty biennially, World Bank (2018) reporting the most recent results. Nowcasting is necessary because, like our estimates of multidimensional poverty, monetary poverty estimates rely on data from household surveys that, in most developing countries, are conducted every 3–5 years. The World Bank's approach to nowcasting relies on covariates of monetary poverty that are observed more frequently, together with assumptions about the evolution of income

or consumption distributions. Specifically, the pass-through of per-capita GDP growth to household income or consumption expenditure is assessed on the basis of historical data for each country. The assumption of distribution-neutral growth since the date of the most recent poverty estimate then allows poverty to be nowcasted on the basis of the most recent growth data. Future projections are conducted under alternative hypothetical scenarios of future growth and its distributional incidence. An application that is related to our research questions is the exploration in World Bank (2018) of the conditions under which the SDG target of reducing extreme monetary poverty to less than 3 percent of the global population might be achieved.

In our present study, with observations at only two time-points for each country, we cannot estimate country-specific stable pass-through from growth or any other covariates to multidimensional poverty. This will, however, be a promising avenue to explore if in the future we have a longer panel. In principle, adopting a covariate-based approach to nowcasting may be less straightforward for multidimensional than monetary poverty, as there is some evidence from cross-country analyses to suggest that multidimensional poverty has a less direct relationship with economic growth than does monetary poverty (Santos *et al.*, 2019). Other covariates may turn out to be better predictors.

Child mortality is another important development indicator, whose estimation is challenging in the absence of well-functioning vital registration systems in many developing countries. Much like our multidimensional poverty measures, estimation therefore relies on periodic household surveys, in this case typically the birth history data collected in DHS and, increasingly, in MICS surveys (UN IGME, 2019). Birth history data yield an annual panel of estimates, often with significant sampling error but also with multiple observations for many periods due to overlap of histories gathered in different surveys. This makes non-parametric modelling of countries' child mortality trajectories feasible, in particular the Bayesian B-spline bias-reduction (B3) model proposed by Alkema and New (2014) and adopted by the UN Inter-agency Group for Child Mortality Estimation. This method can account for sampling and non-sampling errors, and capture short term fluctuations in the mortality rate. In contrast to the monetary poverty nowcasts and forecasts described above, covariates are not used to derive estimates or make projections. However, non-parametric methods are hardly feasible in our study because, in contrast to the data available to estimate child mortality, we have only two observations available for each country. We are thus forced to rely on simpler parametric methods, using cross-country variation to identify plausible parametric trajectory models for multidimensional poverty.

The monitoring of child malnutrition (latest results in JCME, 2020) again relies on similar surveys. In this case, like in our study, the number of observations for each country is

relatively low. Assessment of each country's progress is computed as its average annual rate of reduction (AARR) either analytically in the case of two observations, or on the basis of a low-n log-linear regression (WHO-UNICEF, 2017). This imposes the assumption that countries' trajectories each follow an exponential path.

Ram (2020) implements a similar approach to make projections of multidimensional poverty, assessing whether the 34 countries analysed by Alkire *et al.* (2017) are on track to halve the proportion of people in multidimensional poverty between 2015 and 2030, should the annual rates of change reported by Alkire *et al.* persist. We explore and implement a similar approach, among others, in this paper. We make use of the more recent data now available for more countries (Alkire *et al.*, 2020c) and extend to multidimensional poverty as well as its sub-indices, accounting for the relationship between them. However, as we will compellingly show, a more suitable modelling assumption is that countries' trajectories of multidimensional poverty follow logistic rather than exponential paths.

This finding aligns with the results of Klasen and Lange (2012), who show that logistic models capture a remarkable proportion of progress over time and across countries in both child mortality and education indicators (primary completion rate and gender balance). See also the earlier work by Meyer *et al.* (1992) and Clemens (2004) on education. Moreover, Lange (2014) applied similar models to projections of primary and secondary completion as well as literacy rates. In the next section we develop this approach further, adapting it to the specific case of multidimensional poverty and its sub-indices.

4 Modelling Multidimensional Poverty Dynamics

With multidimensional poverty estimates available at just two points in time for each country, we cannot precisely estimate nor forecast individual countries' multidimensional poverty trajectories. Given our data constraints, in this section we explore alternative dynamic models that we may use to implement projections of countries' trajectories. We identify preferred models, which respect theoretical bounds on multidimensional poverty levels and are strongly supported by cross-country evidence on countries' trajectories. We conclude the section by implementing country-specific calibrations of these models.

4.1 Analytical Framework and Notation

4.1.1 Multidimensional Poverty

Multidimensional poverty is measured following the method established by Alkire and Foster (2011), in particular its global MPI implementation described in section 2. The standard exposition (see, for example, Alkire *et al.*, 2015) develops sample estimators appropriate for a simple random sample; we establish the population analogue here.

Given achievements x_{ij} in d indicators $j = 1, 2, \ldots, d$, each of which is assigned a *deprivation cutoff* z_j and *weight* w_j such that $\sum_{j=1}^{d} w_j = 1$, an individual i's *deprivation score* is

$$c_i = \sum_{j=1}^{d} w_j \mathbb{I}(x_{ij} < z_j). \tag{1}$$

Given also a *poverty cutoff* k (which Alkire and Santos, 2014, set to $\frac{1}{3}$ for the global MPI), the individual is considered *multidimensionally poor* if $c_i \geq k$; her *censored deprivation score* $c_i(k) = c_i \mathbb{I}(c_i \geq k)$.

The level of *Multidimensional Poverty* (MPI) in a population is then $M = \mathbb{E}\left(c_i(k)\right)$, the average censored deprivation score in that population.[3] Applying the law of iterated expectations,

$$\begin{aligned} M &= \mathbb{E}\left(c_i(k)|c_i \geq k\right)\mathbb{P}(c_i \geq k) + \mathbb{E}\left(c_i(k)|c_i < k\right)\mathbb{P}(c_i < k) \\ &= \mathbb{E}\left(c_i(k)|c_i \geq k\right)\mathbb{P}(c_i \geq k) + 0 \times \mathbb{P}(c_i < k) \\ &= \mathbb{E}\left(c_i|c_i \geq k\right)\mathbb{P}(c_i \geq k) \\ &= A \times H \end{aligned} \tag{2}$$

where A is the *intensity* of multidimensional poverty $\mathbb{E}\left(c_i|c_i \geq k\right)$, the average deprivation score among the poor, and H is the *incidence* or headcount $\mathbb{P}(c_i \geq k) = \mathbb{E}(\mathbb{I}(c_i \geq k))$. By construction, $H \in [0, 1]$, $A \in [k, 1]$ and $M \in [0, 1]$.

4.1.2 Trajectories

Countries are indexed $s = 1, 2, \ldots, S$. Our objects of interest are countries' time-paths (or *trajectories*) of multidimensional poverty, $M_s(t)$, its intensity $A_s(t)$ and incidence $H_s(t)$. We may write $y_s(t)$ to represent any of these outcomes of interest, or $y(t)$ when we do not refer to a specific country. Time-derivatives are notated with dots, so $\dot{y}(t) = \frac{\mathrm{d}y}{\mathrm{d}t}$.

[3] Following Alkire and Foster (2011), the usual notation is M_0. To simplify notation, we drop the subscript 0 in this paper as we do not use any other members of Alkire and Foster's class of multidimensional indices.

An estimate obtained from microdata will be labelled with a hat, so $\hat{M}_s(t_{s\tau})$ is the estimated level of multidimensional poverty in country s at time $t_{s\tau}$. (As discussed in section 2, we have poverty estimates at two discrete points in time for each country, so $\tau = 1, 2$, but these points in time are different for different countries, thus t must be labelled by s as well as τ). An alternative, abbreviated notation for such estimates, which constitute the observations for our empirical models, is $\hat{M}_{s\tau}$ or even $M_{s\tau}$ (respectively, $H_{s\tau}$, $A_{s\tau}$ and in general $y_{s\tau}$). A projection obtained from a projection model is labelled with a wedge, so, for example, $\check{H}_s(t)$ is the projected incidence in country s at time t (continuous).

We observed above that multidimensional poverty may be decomposed as the product of intensity and incidence; at most two of $M_s(t)$, $A_s(t)$ and $H_s(t)$ can vary independently. Therefore, to ensure consistency, we shall model $M_s(t)$ indirectly as

$$M_s(t) = H_s(t)A_s(t) \tag{3}$$

throughout this paper.

4.1.3 Canonical Dynamic Models

A very simple dynamic model for the trajectory of outcome $y(t)$ is the **linear** model

$$y(t) = \alpha^{\text{lin}} - \beta^{\text{lin}}t \tag{4}$$

in which the rate of change $\dot{y}(t) = -\beta^{\text{lin}}$ is constant. While simple, linear models are rarely used for projections of development indicators; an exception is Nicolai *et al.* (2015) who implemented simple linear projections for many SDG indicators. In the case of multidimensional poverty, a linear model does not respect the bounded nature of all outcomes of interest.

Another simple dynamic model for the trajectory of outcome $y(t)$, which respects a lower bound at 0, is the **exponential** or **constant relative change**[4] model

$$y(t) = e^{\alpha^{\text{crc}} - \beta^{\text{crc}}t} \tag{5}$$

in which the relative rate of change $\frac{\dot{y}(t)}{y(t)} = -\beta^{\text{crc}}$ is constant; equivalently, the rate of change $\dot{y}(t) = -\beta^{\text{crc}}y$ is proportional to y. Note that the log-transformation $\tilde{y}(t) = \ln(y(t)) = \alpha^{\text{crc}} - \beta^{\text{crc}}t$ is linear in the parameters. This is the dynamic model implemented to assess progress in child malnutrition (WHO-UNICEF, 2017) and by Ram (2020) to project the incidence of multidimensional poverty. It is a plausible candidate for trajectories of $H(t)$

[4]Described as *proportional* in Alkire *et al.* (2020b)

and $M(t)$, which are bounded below at 0, and could be adapted for $A(t)$, which is bounded below at k.

A slightly more complex dynamic model for the trajectory of outcome $y(t)$, which respects both lower and upper bounds, is the **logistic model**

$$y(t) = \frac{1}{1 + e^{-\alpha^{\log} + \beta^{\log} t}} \tag{6}$$

in which the rate of change $\dot{y}(t) = -\beta^{\log} y(1-y)$ is quadratic in y, passing through $(0, 0)$ and $(1, 0)$. Note that the logit-transformation $\tilde{y}(t) = \ln\left(y(t)/(1-y(t))\right) = \alpha^{\log} - \beta^{\log} t$ is linear in the parameters. Logistic models were implemented by Klasen and Lange (2012) and Lange (2014) to model child mortality and education indicator dynamics. The logistic model is a plausible candidate for trajectories of $H(t)$ and $M(t)$, which are bounded between 0 and 1, and could be adapted for $A(t)$, which is bounded between k and 1.

Figure 3: Canonical Dynamic Models

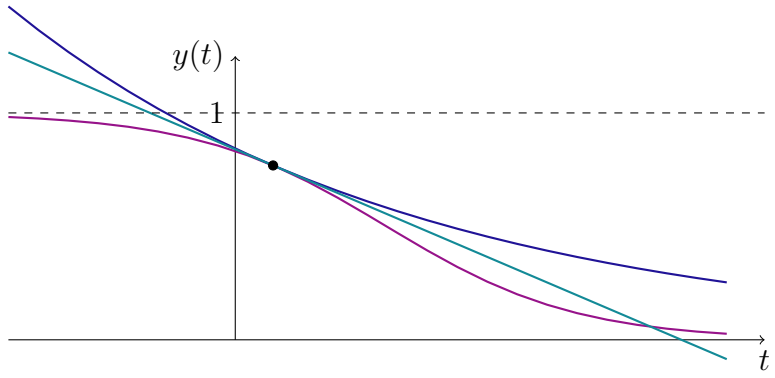

Notes: Linear model —— ; exponential model —— ; logistic model ——.

Several observations are pertinent:

- For each of these models, there is a transformation $\tilde{y}(t) = \alpha - \beta t$ that is linear in the parameters; that shall prove useful in the subsequent empirical modelling.
- In each case, the parameter β represents the rate of change or speed of transition.
- Each model is characterised by a first-order ordinary differential equation (ODE): $\dot{y}(t)$ is constant in the linear model, linear in $y(t)$ in the exponential (constant relative change) model and quadratic in $y(t)$ in the logistic model.

Figure 3 illustrates linear (4), exponential (5) and logistic (6) trajectories calibrated to pass through a particular point with a particular rate of change.

4.2 Cross-Country Evidence on Poverty Dynamics

As noted above, with observations at only two time-points for each country, we cannot estimate or forecast trajectories at country level. We therefore utilise cross-country evidence to inform our choice of projection models.

Figure 4: Cross-Country Evidence

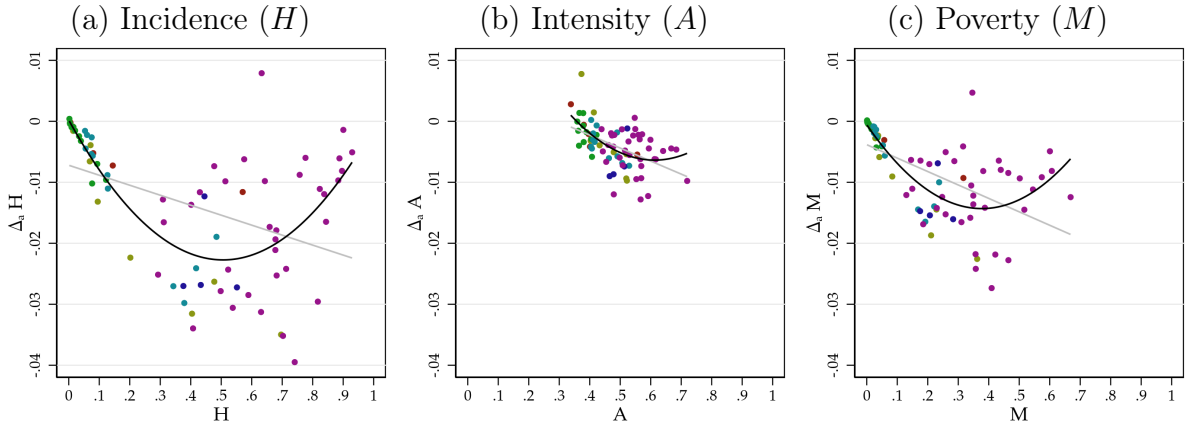

Notes: Own calculations, changes on vertical axis are average annual changes, black line shows quadratic fit, grey line linear fit. Countries are colour-coded by world region: ● Arab States; ● East Asia and the Pacific; ● Europe and Central Asia; ● Latin America and the Caribbean; ● South Asia; ● Sub-Saharan Africa.

For each outcome of interest, Figure 4 illustrates the cross-country relationship between average annual change Δy, a proxy for $\dot{y}(t)$, and level. In the case of H and M, the relationship is clearly nonlinear; in the case of A the pattern is less clear. While countries from different world regions tend to cluster at different levels of the outcomes, the emerging relationship between levels and changes is not driven by one particular world region, but rather supported by countries across the globe. There is, of course, substantial variation across different countries.

To explore the dynamics more systematically, we estimate cross-country models of average annual changes in the outcomes of interest Δy as polynomial functions of levels of the outcomes. As the average annual change is a proxy for $\dot{y}(t)$ at both t_1 and t_2, we retain both observations for each country. We are relaxed about any artificial inflation of sample size, as this exercise is purely for model selection purposes and any effect will have a similar impact on all models.

Table 2 reports results for H, the incidence of poverty. A linear function of H (model 1) is strongly rejected in favour of a quadratic (model 2). Adding a cubic term (model 3) slightly improves the fit, but the cubic coefficient is not significantly different from zero and the improvement in fit is too slight to justify the considerable extra complexity in the dynamic model.[5] Interestingly, a model with H, A and their product (model 4) gives

[5]The corresponding ODE may not have a closed-form solution.

equally good fit, and adding H^2 (model 5) even better, but again, the slight gain does not outweigh the considerable extra modelling complexity. We conclude that the quadratic model $\dot{H}(t) = aH^2 + bH + c$ is most appropriate.

Table 2: Dynamic Model Selection for $H(t)$

	(1) ΔH	(2) ΔH	(3) ΔH	(4) ΔH	(5) ΔH
H	-0.0148***	-0.0918***	-0.127***	-0.161***	-0.131***
	(-5.24)	(-11.80)	(-6.42)	(-11.53)	(-7.13)
H^2		0.0966***	0.203***		0.0562*
		(10.31)	(3.63)		(2.48)
H^3			-0.0810		
			(-1.93)		
A				-0.0497	0.00864
				(-1.96)	(0.25)
HA				0.269***	0.117
				(9.60)	(1.73)
Constant	-0.00816***	-0.00106	0.000492	0.0163	-0.00489
	(-6.34)	(-0.87)	(0.34)	(1.62)	(-0.37)
Observations	160	160	160	160	160
Adjusted R^2	0.143	0.486	0.494	0.496	0.512

Notes: Own calculations, t-statistics in parentheses, indicated levels of significance are * $p < 0.05$, ** $p < 0.01$, *** $p < 0.001$. See A.1 for the list of datasets underlying these results.

Recalling that the characteristic ODE for the logistic dynamic model is $\dot{y}(t) = -\beta y(1-y)$, this is equivalent to the quadratic coefficients satisfying $a + b = 0$ and $c = 0$. The p-value for a Wald test of the joint hypothesis is 0.2078; we fail to reject it and so conclude that the logistic model (equation 6, illustrated in Figure 5), is most appropriate for $H(t)$.

Figure 5: Dynamic Model for $H(t)$

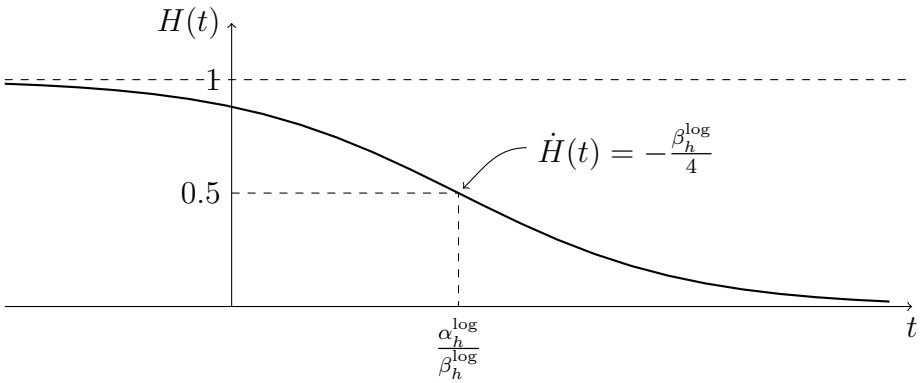

Note: Own analysis. Illustration of logistic trajectory with parameter roles illustrated through identification of time, level and rate of change at the point of inflection.

As is clear in Figure 4, the relationship between changes in A, the intensity of poverty,

and its level, is less strong than for H or M. Table 3 reports results for regressions of ΔA on polynomial functions of A and H. A linear function of A (model 1) explains only 18% of the variation in ΔA and adding the quadratic term (model 2) increases that to just 21%. Interestingly, H has similar explanatory power (models 3 and 4), and a model with A, H and their product (model 5) slightly more. But the gain is marginal over model (2). Despite the small difference in explanatory power between models (1) and (2) we prefer the quadratic function, which corresponds to a logistic trajectory, over the linear function, which corresponds to an exponential trajectory. Several countries actually experience increases in intensity of poverty, so it is important that our projection model respects the upper bound on A.

Table 3: Dynamic Model Selection for $A(t)$

	(1) ΔA	(2) ΔA	(3) ΔA	(4) ΔA	(5) ΔA
A	-0.0184***	-0.104***			-0.0276**
	(-5.97)	(-3.39)			(-2.78)
A^2		0.0871**			
		(2.81)			
H			-0.00516***	-0.0131***	-0.0175**
			(-5.94)	(-4.31)	(-3.21)
H^2				0.00991**	
				(2.72)	
HA					0.0330**
					(3.01)
Constant	0.00465**	0.0253***	-0.00222***	-0.00149**	0.00895*
	(3.15)	(3.37)	(-5.59)	(-3.15)	(2.28)
Observations	160	160	160	160	160
Adjusted R^2	0.179	0.213	0.177	0.209	0.220

Notes: Own calculations, t-statistics in parentheses, indicated levels of significance are * $p < 0.05$, ** $p < 0.01$, *** $p < 0.001$. See A.1 for the list of datasets underlying these results.

Given $\dot{A}(t) = aA^2 + bA + c$ (model 2), the p-value for the Wald test of the joint hypothesis $a + b = 0$ and $c = 0$ is indistinguishable from zero; we strongly reject the hypothesis and so cannot adopt the simple logistic model (equation 6) for $A(t)$. This is natural, as A is bounded below at $\frac{1}{3}$ rather than 0. The modified (three-parameter) logistic function that respects the bounds at $\frac{1}{3}$ and 1 is characterised by the ODE $\dot{A}(t) = \frac{1}{2}\beta(3A^2 - 4A + 1)$, which is equivalent to the quadratic coefficients satisfying $a = 3c$ and $b + 4c = 0$. The p-value for a Wald test of the joint hypothesis is 0.4990; we fail to reject it and conclude that the modified logistic model

$$y(t) = \frac{1 + 3e^{\alpha^{\text{ml}} - \beta^{\text{ml}} t}}{3(1 + e^{\alpha^{\text{ml}} - \beta^{\text{ml}} t})}, \tag{7}$$

illustrated in Figure 6, is most appropriate for $A(t)$. In this case, the modified logit-transformation $\tilde{y}(t) = \ln\left((3y(t) - 1)/3(1 - y(t))\right) = \alpha^{\text{ml}} - \beta^{\text{ml}}t$ is linear in the parameters.

Figure 6: Dynamic Model for $A(t)$

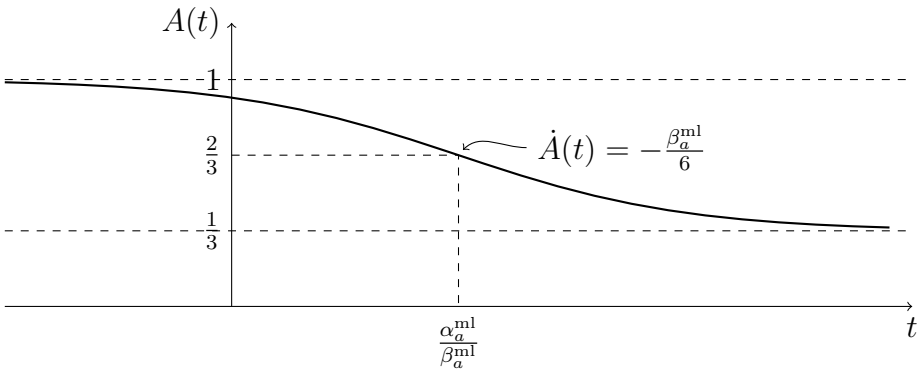

Note: Own analysis. Illustration of modified logistic trajectory with parameter roles illustrated through identification of time, level and rate of change at the point of inflection.

Finally, we turn to dynamic model selection for $M(t)$, reported in Table 4. As noted above, $M(t) = H(t)A(t)$, so $\dot{M}(t) = \dot{H}(t)A(t) + H(t)\dot{A}(t)$. Given our preferred models for $H(t)$ and $A(t)$, we thus expect $\dot{M}(t)$ to be a polynomial function of H, HA, H^2A and HA^2. Such a function (model 1) explains 54% of the variation in ΔM. We may ask whether modelling $\dot{M}(t)$ as a function of H and A performs any better than as a function of M itself; model (1) does indeed explain more of the variation in ΔM than polynomial functions of M (models 2–4). This reassures us that our approach to modelling $M(t)$ is appropriate.

4.3 Assessment of the Dynamic Models

We established in section 4.2 above that the logistic model (6) is supported by both theoretical bounds and cross-country empirical evidence as the preferred model for the incidence of multidimensional poverty, $H(t)$. Similarly, the modified logistic model (7) is supported by theoretical bounds and, to a lesser extent, by cross-country empirical evidence as the preferred model for the intensity of multidimensional poverty, $A(t)$.

The model-selection exercise above allowed us to identify our preferred parametric models, but relied on the approximation of taking Δy as a proxy for $\dot{y}(t)$ for each variable. Having identified the preferred parametric models, we may now estimate their parameters and assess model fit with properly-specified models.

Table 4: Dynamic Model Selection for $M(t)$

	(1) ΔM	(2) ΔM	(3) ΔM	(4) ΔM
H	-0.210***			
	(-3.81)			
HA	0.581**			
	(3.08)			
H^2A	0.0310			
	(1.59)			
HA^2	-0.464**			
	(-2.92)			
M		-0.0213***	-0.0750***	-0.124***
		(-7.72)	(-10.71)	(-7.70)
M^2			0.108***	0.343***
			(8.13)	(4.82)
M^3				-0.271***
				(-3.36)
Constant	0.0000438	-0.00440***	-0.00133	-0.0000559
	(0.06)	(-6.25)	(-1.90)	(-0.07)
Observations	160	160	160	160
Adjusted R^2	0.539	0.269	0.482	0.514

Notes: Own calculations, t-statistics in parentheses, indicated levels of significance are * $p < 0.05$, ** $p < 0.01$, *** $p < 0.001$. See A.1 for the list of datasets underlying these results.

Recall that each of the models considered above could be expressed in a transformed version $\tilde{y}(t) = \alpha - \beta t$ that is linear in the parameters β, which represents speed or rate of poverty reduction, and α, which, given β, represents temporal location of the trajectory. We assume that β is fixed across all countries, but allow α to vary. This yields the model

$$\tilde{y}_{s\tau} = \alpha_s - \beta t_{s\tau} + \varepsilon_{s\tau} \qquad \forall s = 1...S; \tau = 1, 2 \tag{8}$$

where $\tilde{y}_{s\tau}$ is the appropriately transformed outcome of interest for country s at time $t_{s\tau}$, α_s are country fixed effects and ε_{st} are idiosyncratic error terms.

Applying the within transformation,

$$\tilde{y}_{s\tau} - \bar{y}_s = -\beta(t_{s\tau} - \bar{t}_s) + (\epsilon_{s\tau} - \bar{\epsilon}_\tau) \qquad \forall s = 1...S; \tau = 1, 2 \tag{9}$$

where $\bar{y}_s$, $\bar{t}_s$ and $\bar{\epsilon}_\tau$ are within-country averages of the transformed outcome, time-points, and error terms, respectively, allows us to arrive at an estimable form of (8). Moreover, an intercept fixed across countries, μ, can be introduced in (9) by adding the pooled mean

of $\tilde{y}_{s\tau}$ (denoted as $\bar{\tilde{y}} \equiv \bar{\alpha} - \beta\bar{t} + \bar{\epsilon}$) to both sides of the equation such that

$$\tilde{y}_{s\tau} - \bar{y}_s + \bar{\tilde{y}} = \mu - \beta(t_{s\tau} - \bar{t}_s + \bar{t}) + (\epsilon_{s\tau} - \bar{\varepsilon}_\tau + \bar{\varepsilon}) \qquad \forall s = 1...S; \tau = 1, 2 \tag{10}$$

where $\mu = \bar{\alpha}$, thus corresponding to the average of the country-fixed effects. An OLS fit of (10) yields the within-estimates of β and μ, and its coefficient of determination corresponds to the within-R^2 goodness of fit measure of the fixed-effects model (8).

Table 5: Fixed-effects estimation results (75 countries)

	(1) H^{lin}	(2) H^{crc}	(3) H^{log}	(4) A^{lin}	(5) A^{crc}	(6) A^{log}
$\hat{\beta}$	0.0138***	0.0616***	0.0934***	0.0040***	0.0081***	0.0164***
	(14.2623)	(13.8100)	(22.8832)	(14.2527)	(14.0851)	(14.2507)
$\hat{\mu}$	0.1912***	-2.5102***	-2.3011***	0.4247***	-0.8599***	-0.3071***
	(15.7763)	(-44.9450)	(-44.9258)	(120.3718)	(-119.9381)	(-21.2544)
R^2	0.64	0.62	0.80	0.63	0.62	0.63
N	150	150	150	150	150	150

Notes: Own calculations, t-statistics in parentheses, indicated levels of significance are * $p < 0.05$, ** $p < 0.01$, *** $p < 0.001$. See A.1 for the list of datasets underlying these results.

We estimate and assess the fit of three alternative dynamic models for H and three for A: linear (4), exponential (5) and logistic (6). Estimation results are reported in Table 5. While the estimates of μ and β are not directly comparable across models, the (within-)R^2 is. These results confirm the logistic model (column 3) as the best dynamic model for $H(t)$; even without allowing β to vary across countries, this model explains 80% of the within-country variation in incidence of multidimensional poverty. Nevertheless, we shall also implement linear and exponential projection models, for comparison of results.

Results for $A(t)$ (columns 4–6) are less clear-cut; all models explain a similar amount of the within-country variation in intensity of poverty over time. In our applications, as discussed in section 4.2, we shall restrict attention to the modified logistic model, which respects the theoretical bounds on intensity.

4.4 Calibration of Projection Model Parameters

The dynamic models developed above account for a remarkable proportion of the changes in multidimensional poverty across the countries in our dataset. Of course, there remains significant unexplained variation across countries, so in order to implement projections for individual countries we calibrate the model parameters separately for each country. As each of our models is an two-parameter model that may be linearised in the parameters, this is straightforward.

4.4.1 Logistic Projection Models

Given incidence and intensity estimates H_{s1}, A_{s1} and H_{s2}, A_{s2} for country s at t_{s1} and t_{s2}, its calibrated parameters $\check{\alpha}^{\log}_{hs}$, $\check{\beta}^{\log}_{hs}$, $\check{\alpha}^{\mathrm{ml}}_{as}$ and $\check{\beta}^{\mathrm{ml}}_{as}$ solve

$$H^{\log}(t_{s\tau}; \check{\alpha}^{\log}_{hs}, \check{\beta}^{\log}_{hs}) = \frac{1}{1 + e^{-\check{\alpha}^{\log}_{hs} + \check{\beta}^{\log}_{hs} t_{s\tau}}} = H_{s\tau}, \qquad \tau = 1, 2,$$

and

$$A^{\mathrm{ml}}(t_{s\tau}; \check{\alpha}^{\mathrm{ml}}_{as}, \check{\beta}^{\mathrm{ml}}_{as}) = \frac{1 + 3e^{\check{\alpha}^{\mathrm{ml}}_{as} - \check{\beta}^{\mathrm{ml}}_{as} t_{s\tau}}}{3(1 + e^{\check{\alpha}^{\mathrm{ml}}_{as} - \check{\beta}^{\mathrm{ml}}_{as} t_{s\tau}})} = A_{s\tau}, \qquad \tau = 1, 2.$$

The calibrated projection models for incidence, intensity and level of multidimensional poverty are then

$$\begin{aligned} \check{H}^{\log}_s(t) =& H^{\log}(t; \check{\alpha}^{\log}_{hs}, \check{\beta}^{\log}_{hs}), \\ \check{A}^{\mathrm{ml}}_s(t) =& A^{\mathrm{ml}}(t; \check{\alpha}^{\mathrm{ml}}_{as}, \check{\beta}^{\mathrm{ml}}_{as}), \quad \text{and} \\ \check{M}^{\log}_s(t) =& \check{H}^{\log}_s(t) \check{A}^{\mathrm{ml}}_s(t). \end{aligned}$$

Parameter calibration and trajectory projection for all three outcomes of interest are illustrated for a hypothetical country in Figure 7 and for India in Figure 8. The coloured dots represent the observations of H, A and M, while the coloured lines represent the calibrated projection models.

Figure 7: Parameter Calibration and Trajectory Projection

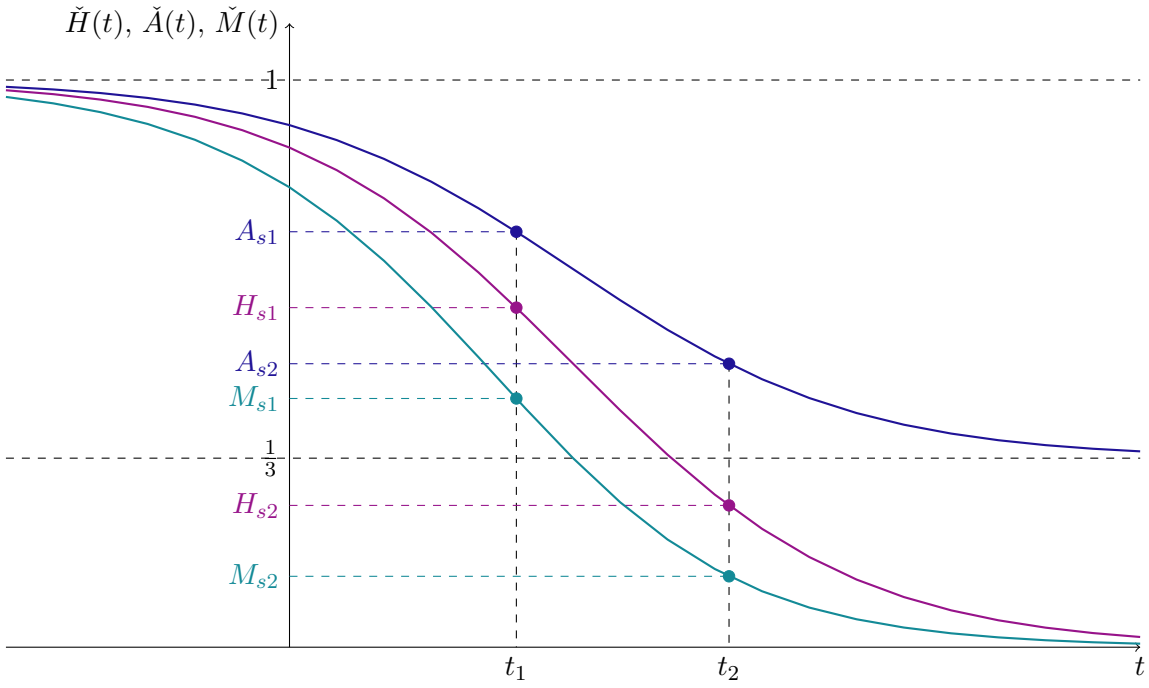

Notes: Illustration of parameter calibration and trajectory projections given hypothetical observations H_{s1}, H_{s2}, A_{s1} and A_{s2}.

Figure 8: Parameter Calibration and Trajectory Projection (India)

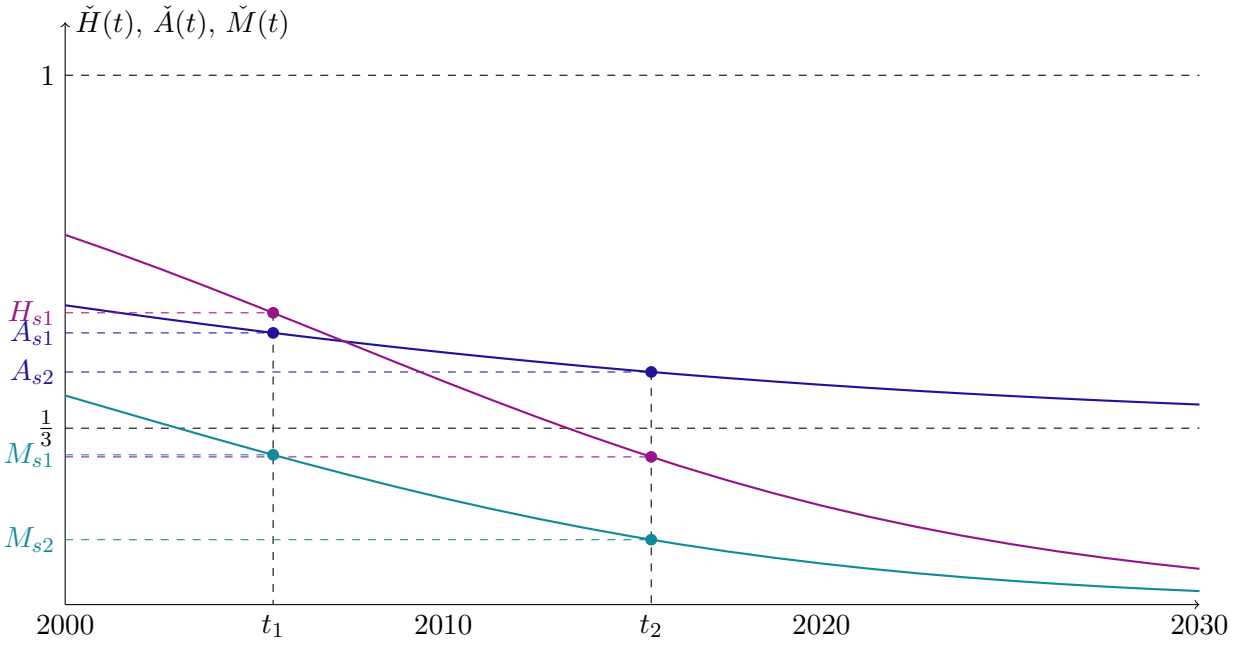

Notes: Illustration of parameter calibration and trajectory projections for India.

The distribution by world region of calibrated parameters $\check{\beta}_{hs}^{\log}$, which represent the speed of poverty incidence reduction, is illustrated in Figure 9. Each country's calibrated parameter is represented by a blue bar. World region medians (circles) and interquartile ranges, which vary across world regions, are illustrated in red. Regional top performers include Sierra Leone in Sub-Saharan Africa, Honduras in Latin America and the Caribbean, and China in East Asia and the Pacific.

Figure 10 illustrates the calibrated logistic model for H by transforming the time variable for each country s by its calibrated parameters, $\tilde{t}_{s\tau}^{\log} = t_{s\tau} - \check{\alpha}_{hs}^{\log}/\check{\beta}_{hs}^{\log}$. This lines up each country's calibrated trajectory such that the point of inflection occurs at $\tilde{t}_{s\tau}^{\log} = 0$, allowing easier comparison across countries. From the figure it is clear that many countries are following similar trajectories, but are at different points along those trajectories. There is some variation, with some countries making faster progress (appearing to follow a steeper curve) while others make slower progress (appearing to follow a shallower curve).

Figure 9: Distribution of $\check{\beta}_{hs}^{\log}$ for logistic model by world region

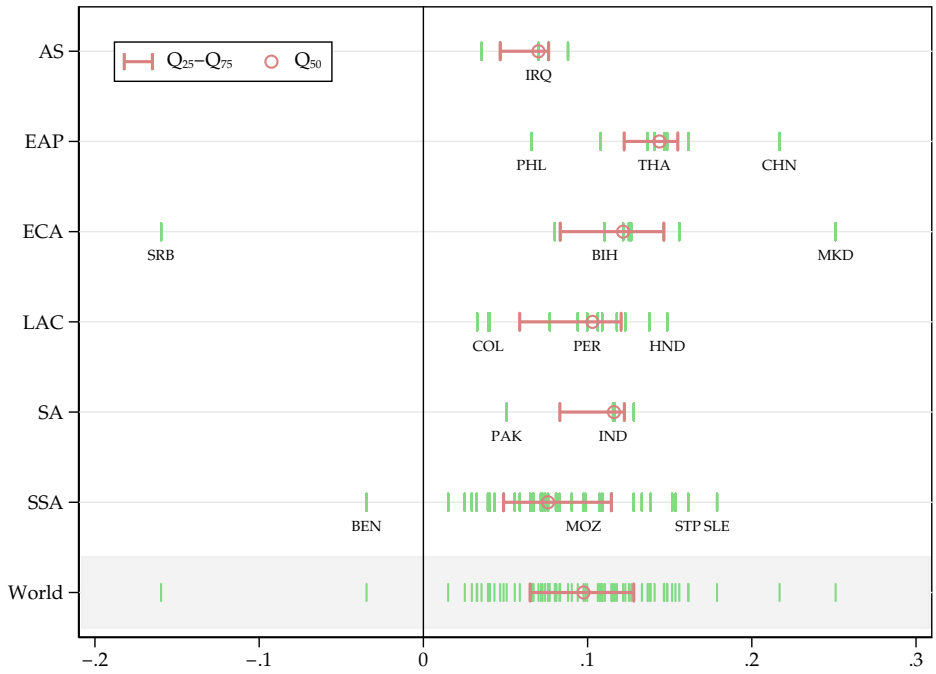

Notes: Blue bars represent a countries' $\check{\beta}_{hs}^{\log}$ as calibrated for the logistic model; world regions are Arab States (AS), East Asia and the Pacific (EAP), Europe and Central Asia (ECA), Latin America and the Caribbean (LAC), South Asia (SA), Sub-Saharan Africa (SSA); only selected countries are labelled for reasons of readability.

Figure 10: Illustration of Calibrated Logistic Model for H

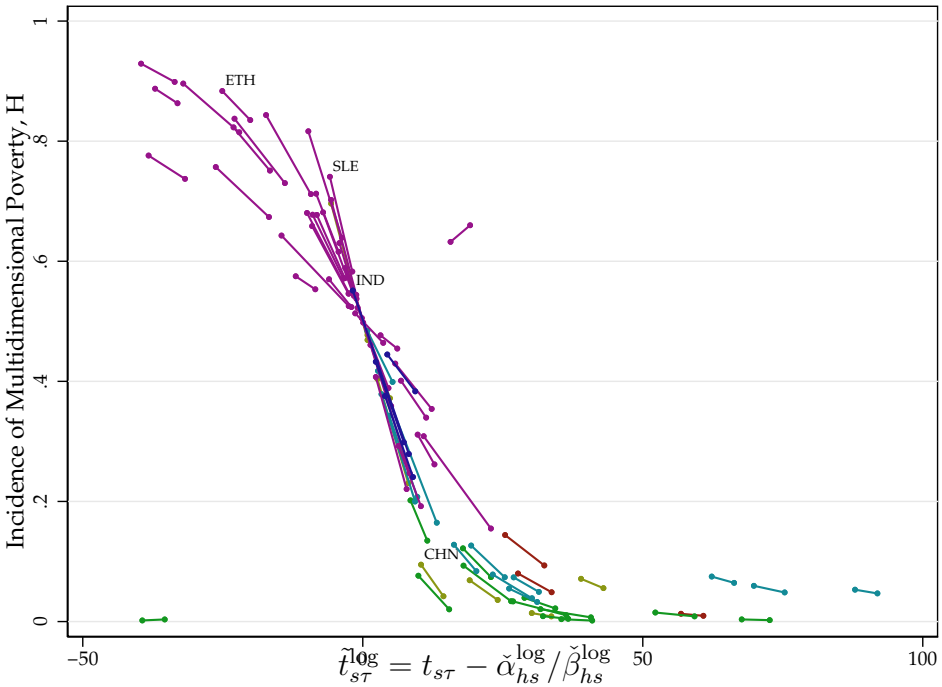

Notes: Incidence of multidimensional poverty, $H_{s\tau}$, against time adjusted according to the calibrated logistic model, $\tilde{t}_{s\tau}^{\log} = t_{s\tau} - \check{\alpha}_{hs}^{\log}/\check{\beta}_{hs}^{\log}$. Selected countries labelled: China (CHN), India (IND), Sierra Leone (SLE) and Ethiopia (ETH). Countries are colour-coded by world region: ● Arab States; ● East Asia and the Pacific; ● Europe and Central Asia; ● Latin America and the Caribbean; ● South Asia; ● Sub-Saharan Africa.

4.4.2 Linear and Exponential Projection Models

While the logistic model for H and modified logistic model for A are our strongly preferred models, we will also implement projections using the linear and exponential models for H. Calibration is analogous to calibration of the logistic models. Given incidence estimates H_{s1} and H_{s2} for country s at t_{s1} and t_{s2}, its calibrated parameters $\check{\alpha}_{hs}^{\text{lin}}$, $\check{\beta}_{hs}^{\text{lin}}$ solve

$$H_{s\tau} = H^{\text{lin}}(t_{s\tau}; \check{\alpha}_{hs}^{\text{lin}}, \check{\beta}_{hs}^{\text{lin}}) = \check{\alpha}_{hs}^{\text{lin}} - \check{\beta}_{hs}^{\text{lin}} t_{s\tau}, \qquad \tau = 1, 2,$$

while $\check{\alpha}_{hs}^{\text{crc}}$ and $\check{\beta}_{hs}^{\text{crc}}$ solve

$$H_{s\tau} = H^{\text{crc}}(t_{s\tau}; \check{\alpha}_{hs}^{\text{crc}}, \check{\beta}_{hs}^{\text{crc}}) = e^{\check{\alpha}_{hs}^{\text{crc}} - \check{\beta}_{hs}^{\text{crc}} t_{s\tau}}, \qquad \tau = 1, 2.$$

The calibrated projection models for incidence and level of multidimensional poverty are then $\check{H}_s^{\text{lin}}(t) = H^{\text{lin}}(t; \check{\alpha}_{hs}^{\text{lin}}, \check{\beta}_{hs}^{\text{lin}})$, $\check{M}_s^{\text{lin}}(t) = \check{H}_s^{\text{lin}}(t)\check{A}_s^{\text{ml}}(t)$, $\check{H}_s^{\text{crc}}(t) = H^{\text{crc}}(t; \check{\alpha}_{hs}^{\text{crc}}, \check{\beta}_{hs}^{\text{crc}})$, and $\check{M}_s^{\text{crc}}(t) = \check{H}_s^{\text{crc}}(t)\check{A}_s^{\text{ml}}(t)$.

Figure 11: Illustration of Calibrated Linear and Exponential Models for H

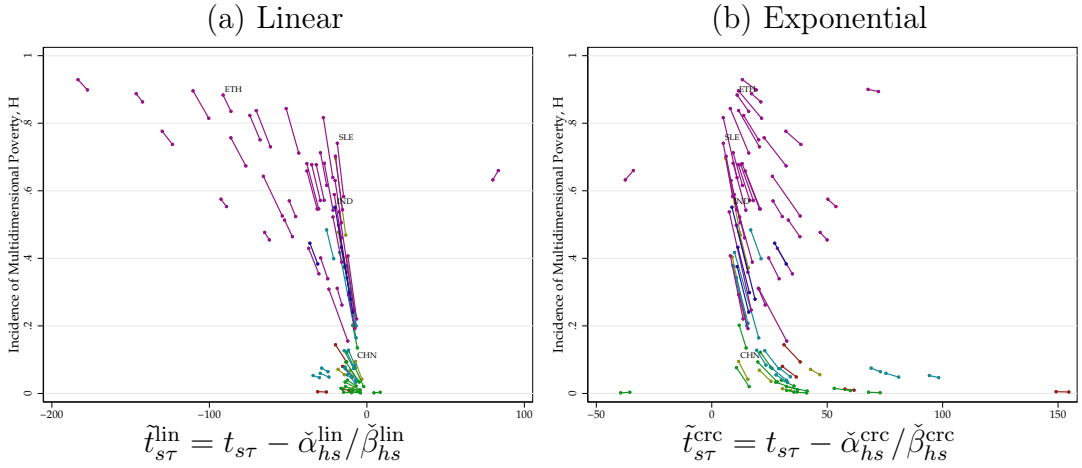

Notes: Incidence of multidimensional poverty, $H_{s\tau}$, against time adjusted according to the calibrated linear model, $\tilde{t}_{s\tau}^{\text{lin}} = t_{s\tau} - \check{\alpha}_{hs}^{\text{lin}}/\check{\beta}_{hs}^{\text{lin}}$, and exponential model, $\tilde{t}_{s\tau}^{\text{crc}} = t_{s\tau} - \check{\alpha}_{hs}^{\text{crc}}/\check{\beta}_{hs}^{\text{crc}}$. Selected countries labelled: China (CHN), India (IND), Sierra Leone (SLE) and Ethiopia (ETH). Countries are colour-coded by world region: ● Arab States; ● East Asia and the Pacific; ● Europe and Central Asia; ● Latin America and the Caribbean; ● South Asia; ● Sub-Saharan Africa.

Figure 11 illustrates the calibrated linear and exponential models for H by transforming the time variable for each country s by its calibrated parameters, $\tilde{t}_{s\tau}^{\text{lin}} = t_{s\tau} - \check{\alpha}_{hs}^{\text{lin}}/\check{\beta}_{hs}^{\text{lin}}$ and $\tilde{t}_{s\tau}^{\text{crc}} = t_{s\tau} - \check{\alpha}_{hs}^{\text{crc}}/\check{\beta}_{hs}^{\text{crc}}$ respectively. In the linear case this lines up each country's calibrated trajectory such that H reaches zero at $\tilde{t}_{s\tau}^{\text{lin}} = 0$, and in the exponential case such that H passes through 1 at $\tilde{t}_{s\tau}^{\text{crc}} = 0$, allowing easier comparison across countries. There is less congruence of trajectories for these models than the logistic model illustrated above in Figure 10.

5 Projection Results

This section implements projections of the global MPI using the models developed in the previous section. To explain the three models in tandem, let us illustrate our results by showing the projected trajectories of poverty reduction for three countries with very distinct poverty levels as per the most recent observations, are at different stages in their trajectories, and are located in different regions: Ethiopia (high poverty and early stage), India (mid poverty and mid stage), and China (low poverty and advanced stage).

Figure 12 depicts the trajectories for these countries based on each model, and clearly shows that they all cross the corresponding observed poverty levels. All three models imply very similar projected poverty levels *between* the observed points, which is particularly true for low and high poverty countries. Projections outside of this range—either further back to the past or into the future—vary more considerably depending on the chosen model. For instance, projections *for high poverty countries* based on the linear and CRC models tend to be more pessimistic about poverty levels in the future compared to logistic model-based projections. This is because, unlike the logistic model, the linear and CRC models fail to anticipate any improvement in the pace of poverty reduction.

Conversely, projections based on linear models tend to be more optimistic about future poverty levels *in mid poor countries* compared to logistic and CRC model-based projections. In fact, the linear projections regularly anticipate a nil poverty level for some mid poor countries, while achieving zero poverty is impossible at any finite point in time for logistic and CRC model-based projections.

Thus, whether or not a country can be expected to meet the target of halving poverty by 2030 may critically depend on the underlying model choice, and yet it is remarkable to find that in many instances, all three models yield identical qualitative results. To see this, note that the horizontal dashed lines in Figure 12 indicate the country's target value for halving poverty between 2015 and 2030; India and China would meet this target according to all three models, whereas Ethiopia would not meet the target under any model if recent trend continue. However, such clear results are not found for every country; in some instances, our assessment of achieving the poverty target is inescapably model-dependent.

Figure 13 presents the full set of results, which show the expected progress in poverty reduction for all 75 countries if observed trends continue. Figure 13 contains the projected 2030 MPI levels obtained by all three models, namely logistic (red lines), linear (green dot), and CRC (purple dot). If all three coloured dots are below the black line for any country, then we can state that it is on track to halve poverty—as measured by MPI—between 2015 and 2030 regardless of the considered model. This powerful result holds for

Figure 12: Projections for Ethiopia (ETH), India (IND), and China (CHN) (different models)

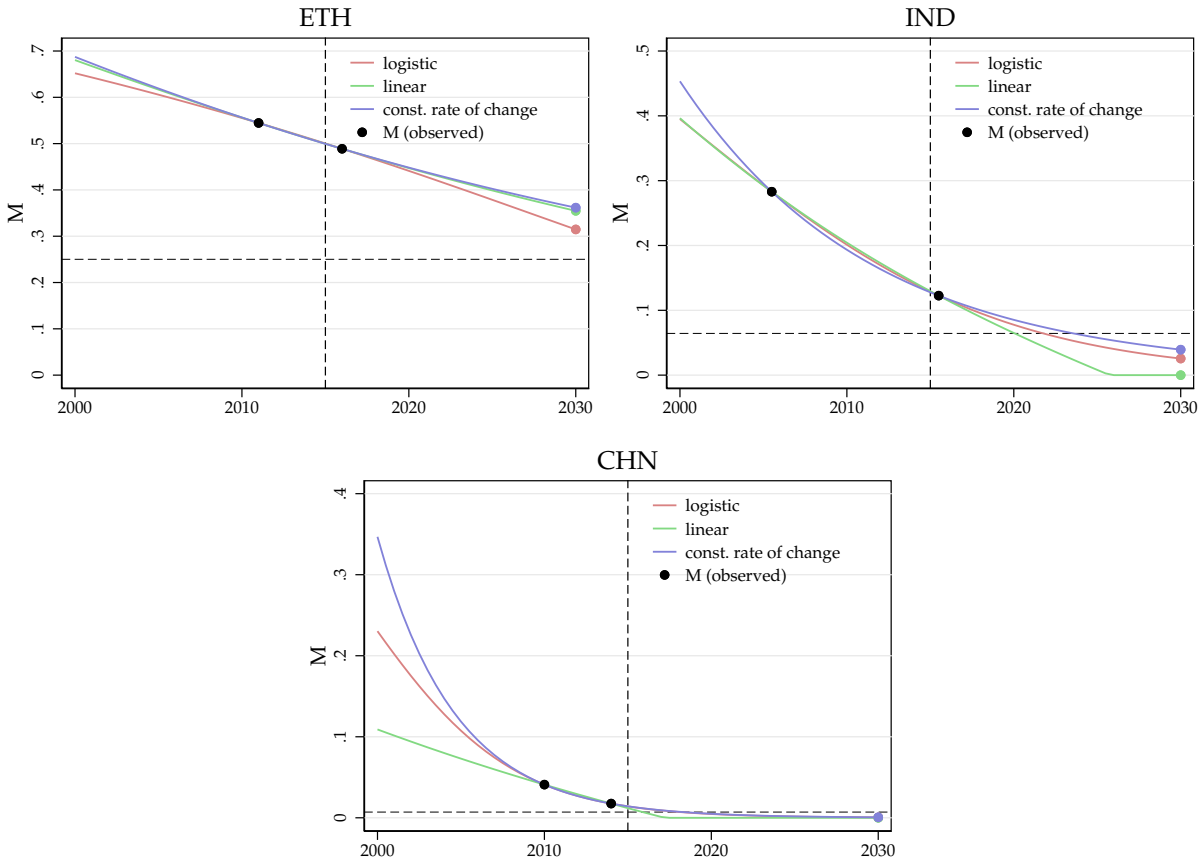

Notes: Authors' calculations, vertical dashed line at 2015; horizontal dashed line at 50% of M_0 in 2015 according to logistic model.

47 out of the 75 countries. All these findings are also summarized in Table 6, and more details for each country can be found in Tables A.2 and A.3.

Conversely, if all three coloured dots are above the black line, then the country is off track to halve poverty regardless of the considered model. If observed trends continue, this is the case of 18 out of the 75 countries. Fourteen of these off-track countries, all in Africa, are among the poorest, suggesting that they will require a significant boost of resources and actions in order to halve poverty.

For 10 countries, our results are model-dependent; they may or may not halve poverty by 2030, depending on which model is posited to represent their poverty dynamics. Nevertheless, 9 of these countries would effectively halve poverty if recent linear trends continued. This positive result arising in light of the linear model is unsurprising given that most of these countries are around the mid stage of their respective trajectories in terms of poverty reduction (see Figure 12).

Importantly, by definition, we measure multidimensional poverty by the MPI, as this

adjusted headcount ratio simultaneously accounts for both incidence and intensity of poverty. However, it is also informative to assess progress in poverty reduction only in terms of the simple poverty headcount ratio (i.e. H). Although it is just a partial index of multidimensional poverty, this ratio has the advantage of being familiar in many poverty analyses. Table 6 also provides results for the simple headcount ratio, showing that 43 countries will be on track to having the incidence of multidimensional poverty, whereas 18—the same ones as in our MPI analysis—would be off track.

Figure 13: MPI projections for 2015–2030 (if observed trends continue)

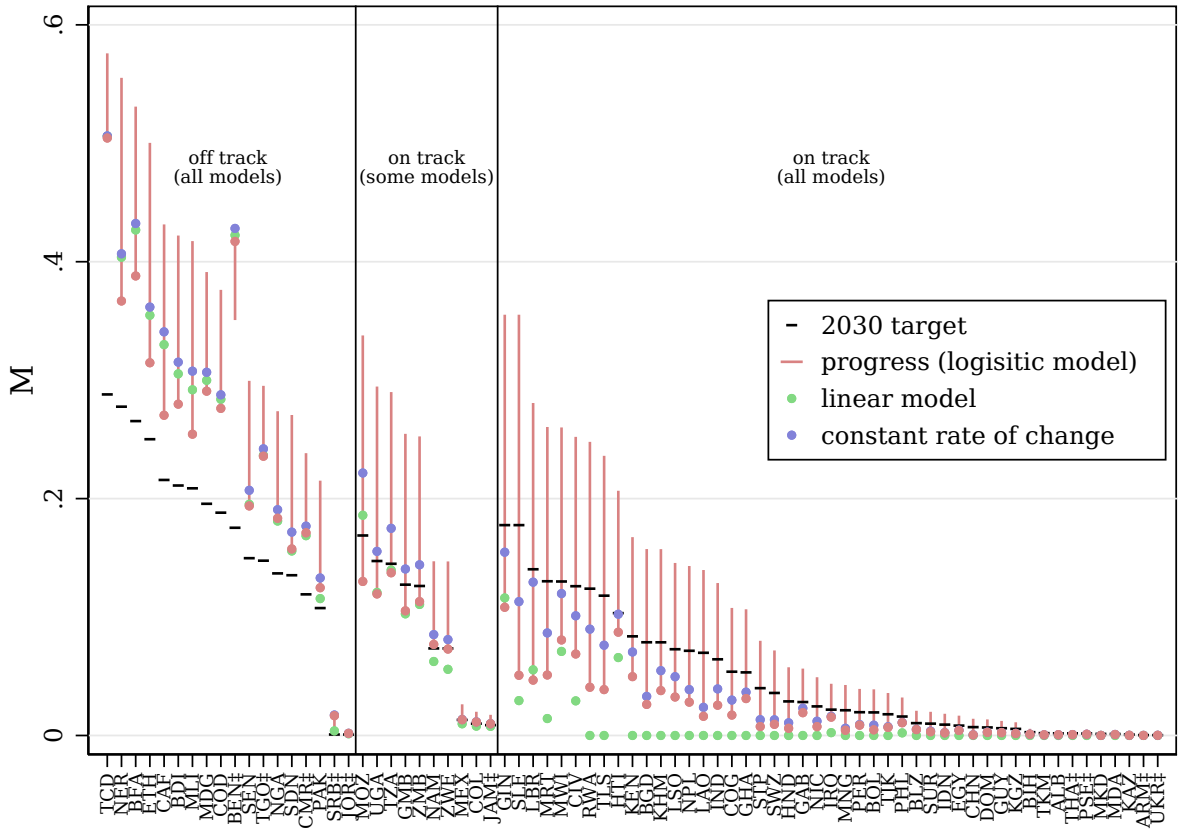

Notes: Authors' calculations; ‡ indicates that estimated change is not significantly different from 0.

Once we have established whether or not each country is expected to meet the poverty target by 2030 if observed trends continue, it is necessary to stress-test these results. An informative analysis for policy actions against poverty consists of identifying meaningful counterfactual trajectories for each country defined by alternative model parameters, different than those actually obtained through calibration (i.e. β, α). This allows us to examine what would happen if poverty followed a different trajectory from the most recent observed poverty level onward. This analysis is useful to assess the sensitivity of results to calibrated parameters. On the one hand, it gives an idea of what kind of performance would be required for a country to meet the poverty target by 2030. On the other hand, it shows the extent to which countries that are expected to meet the target given their

Table 6: Number of countries target met status and model

(a) Adjusted headcount ratio (MPI)

Robust to model	CRC		Linear		Logistic	
	Not met	Met	Not met	Met	Not met	Met
No	10		1	9	4	6
Yes	18	47	18	47	18	47
Total	28	47	19	56	22	53

(b) Headcount ratio

Robust to model	CRC		Linear		Logistic	
	Not met	Met	Not met	Met	Not met	Met
No	14		2	12	6	8
Yes	18	43	18	43	18	43
Total	32	43	20	55	24	51

Notes: Authors' calculation.

observed performance are at risk of missing it if their observed pace of poverty reduction decreases.

Based on its theoretical adequacy and good empirical fit, we focus on the logistic model for these counterfactual analyses. To identify a parsimonious set of meaningful alternative calibrations, we consider the empirical joint distribution of $\hat{\alpha}^{log}$ and $\hat{\beta}^{log}$ across countries to define 'median' performance as a logistic trajectory of MPI corresponding to the median values of both parameters. In a similar way, we define 'lower quartile' and 'upper quartile' performance, and interpret them as benchmarks of plausible (i.e. realistic in the sense that other countries demonstrate similar levels of) 'slow' and 'good' performance, respectively.

To illustrate this, let us revisit the trajectories of MPI for Ethiopia (a high poverty, early stage country) and India (a mid poverty, mid stage country). Figure 14 shows that Ethiopia's observed performance in poverty reduction (red line) is close to being a 'median' performance in our dataset (blue dashed line). Given its observed performance (i.e. with nationally calibrated model parameters), Ethiopia is not expected to meet the target by 2030, but this would be achievable under an 'upper quartile' performance. This is a powerful result because it shows that meeting the target may be feasible even for a large country with one of the most challenging poverty conditions globally.

Turning now to India, Figure 14 shows that it is the typical 'upper quartile' performing country in our dataset, and it is expected to meet the target by 2030 of observed trends continue. Exploring different counterfactual trajectories, we find that India can be expected to halve poverty by 2030 even if its performance is pushed down to a 'median' *and* even a 'lower quartile' performance in poverty reduction. This result is of interest because even though there was remarkable performance in terms of poverty reduction in

2005/6 to 2015/16 Alkire *et al.* (2018), that period ended close to the start of the fifteen year period under study.

Figure 14: Projections for Ethiopia (ETH) and India (IND) under counterfactual performance levels

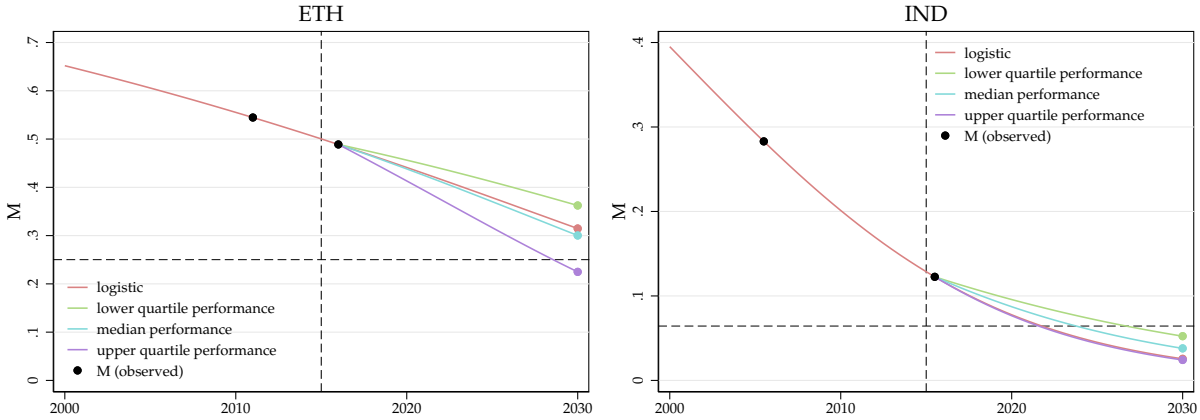

Notes: Authors' calculations, vertical dashed line at 2015; horizontal dashed line at 50% of M_0 in 2015 according to logistic model.

Turning now to all 75 countries in our dataset, Figure 15 shows the results under counterfactual performance in two panels for increased visibility: panel (a) depicts high poverty countries, and panel (b) low poverty countries. We posit 'median' performance in terms of poverty reduction (yellow dots) as a meaningful benchmark for countries that are found to be off track according to projections by the logistic model. This regularly implies a moderate (i.e. realistic) improvement in their observed performance. For countries that are found to be on track according logistic model-based projections, it is important to note that, normally, they already perform at a level corresponding to 'median' performance or better. Thus we consider 'lower quartile' performance as an appropriate counterfactual benchmark (green dots) for these countries.

Recall that 22 countries that are off track to meet the target by logistic model-based projections (see Table 6), 18 of which were off track by all three considered models, plus 4 additional countries where models disagree. Fifteen of them (10 high poverty, 5 low poverty) would manage to achieve this goal if they boost their poverty reduction performance to a 'median' level. These results show that relatively slow trajectories of poverty reduction are not pre-determined; there is a chance to increase the likelihood of halving poverty by 2030 if some of the countries shifted gear. However, Figure 15 also makes it visible that the challenge is greater some of the poorest countries, which are all in Africa, as these would not halve poverty by 2030, even if current performance were boosted.

Conversely, we also find that several countries among the 53 that would be expected to meet the target according to the logistic model-based projections if observed trends

Figure 15: MPI projections for 2015–2030 for alternative scenarios

(a) high poverty countries

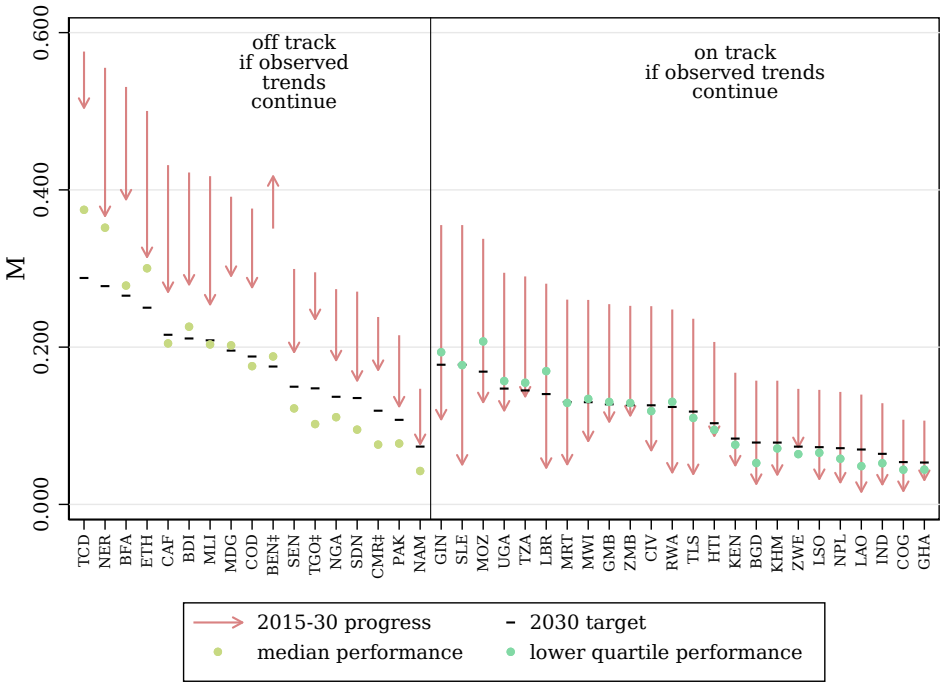

(b) low poverty countries

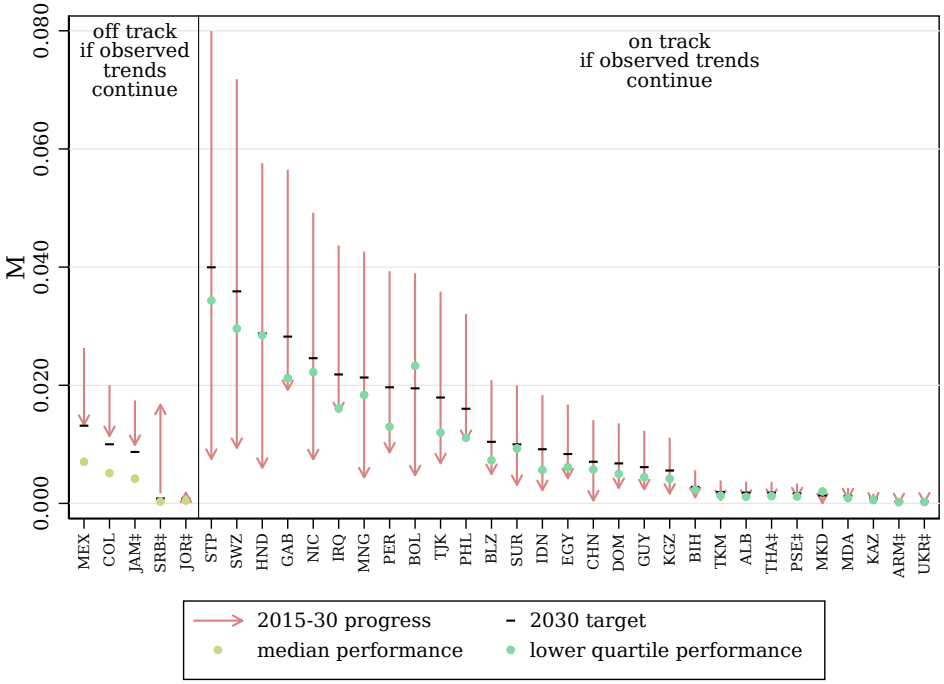

Notes: Authors' calculations; projected 2015–2030 progress is based on logistic model; ‡ indicates that the estimated change for a country is not significantly different from 0.

continue are actually at risk of failing to halve poverty if their poverty reduction dynamics are interrupted. This is the case of 9 high poverty countries and 2 low poverty countries. These results are as important as the previous ones in the sense that they offer compelling evidence for the need of continuity and sustainability of policy efforts in the quest to halve poverty by 2030.

6 The Impact of COVID-19 on Multidimensional Poverty

The COVID-19 pandemic spread rapidly throughout the world in the early months of 2020 and is anticipated to have significant impacts on multidimensional poverty levels and trends, disrupting the projections developed above. Real world data are not yet available to measure the impact of the pandemic on multidimensional poverty, so we conduct micro-simulations at the country level, which we then combine with our projection models to determine the potential impact on global multidimensional poverty in 2020. This enables us to assess the potential setback in years of poverty reduction on the global level due to the COVID-19 pandemic.

6.1 Microsimulations of COVID-19 Impact

Initial microsimulations were implemented using the underlying micro datasets of the global MPI 2020 (Alkire, Kanagaratnam, and Suppa, 2020b), which cover 107 countries. Ten of these countries, however, lack the nutrition indicator, which is essential for our simulations.[6] We therefore implemented the microsimulations for the remaining 97 countries. For a list of these countries and the underlying datasets, see Table A.1 of the appendix. In order to determine the potential impact of the pandemic on multidimensional poverty in 2020 we need to combine the microsimulation results with results of our projection models (section 5), so our analysis in section 6.3 below will focus on those 70 countries that both include the nutrition indicator and for which we have projection results. A detailed explanation of the assumptions behind our microsimulations is presented in Appendix B.

The currently unfolding COVID-19 pandemic is impacting the lives and livelihoods of people across the globe in numerous ways. Considering the indicators of multidimensional poverty as measured by the global MPI, we expect substantial impacts through two that are being severely affected by the pandemic—nutrition and children's school attendance.[7]

[6] Relevant information for the nutrition indicator is not collected in the surveys of Afghanistan, Brazil, Colombia, Cuba, Dominican Republic, Indonesia, Papua New Guinea, Philippines, Ukraine or Viet Nam.

[7] The COVID-19 pandemic is also likely to have medium- and long-term impacts on other global MPI indicators. For example, child mortality is anticipated to increase where health systems are disrupted (Roberton *et al.*, 2020).

A common policy response to the COVID-19 pandemic across countries of all levels of development has been to close schools as a part of national or local lockdowns. UNESCO data suggest that school closures peaked in April 2020, with over 91 percent of the world's learners out of school. Subsequently, however, this proportion fell gradually to just over 60 percent in July 2020.[8]

In order to simulate the shock to school attendance, we assume that 50 percent of children attending school experience continued interruption to school attendance, which can be considered a conservative assumption allowing for moderate improvements over the remainder of 2020. More specifically, we randomly draw 50% of those children, who given their age should attend primary school. This procedure takes both country-specific entry age and duration of primary schooling into account.[9] If a child is selected not to attend school, the entire household is considered deprived in school attendance, which follows the indicator definition of the global MPI.[10]

The COVID-19 pandemic has also disrupted livelihoods and food supply chains globally. The World Food Programme (WFP) estimates that the number of people facing acute food insecurity may increase by 130 million across 55 countries (WFP, 2020). Extending this to all 70 countries covered in our analysis, we anticipate that around 25 percent of people who were multidimensionally poor or vulnerable but who were not undernourished before the pandemic may become undernourished.[11] We focus on those who were vulnerable or already poor, to account for their elevated risk of experiencing such a disruption. We consider this a moderate scenario for simulating the potential impact of the pandemic on the nutrition indicator.

In order to simulate the shock to nutrition we randomly draw 25% of those individuals who are either vulnerable to multidimensional poverty or are already multidimensionally poor, but do not suffer from undernutrition. If an individual is selected to suffer from undernutrition, their entire household is considered to be deprived in the nutrition indicator, which follows the respective indicator definition of the global MPI.[12]

[8]Data accessed via https://en.unesco.org/covid19/educationresponse on 2 July 2020, see also UNESCO (2020).

[9]Data on entrance age and duration of primary school is provided by UNESCO under http://data.uis.unesco.org/.

[10]Note that, for each child selected, there may or may not result an increase in multidimensional poverty, but it cannot decrease. If the child's household has no other deprivations then the school attendance deprivation is not sufficient for it to reach the threshold to be considered multidimensionally poor. If there had already been a child in the household in the relevant age bracket who was out of school, the household would already have been deprived in school attendance and so deprivation according to the indicator definition of the global MPI will not increase.

[11]A household is considered to be vulnerable to multidimensional poverty as measured by the global MPI if its weighted deprivation count is between 20–33% of the maximum possible deprivations (see e.g. Alkire *et al.*, 2020b,a).

[12]Note that there may or may not result an increase in multidimensional poverty, but it cannot decrease.

Figure 16: Simulated Impact of COVID-19 on Multidimensional Poverty

(a) Upper Impact on Nutrition (50%)

(i) With School Attendance (50%) (ii) Without School Attendance

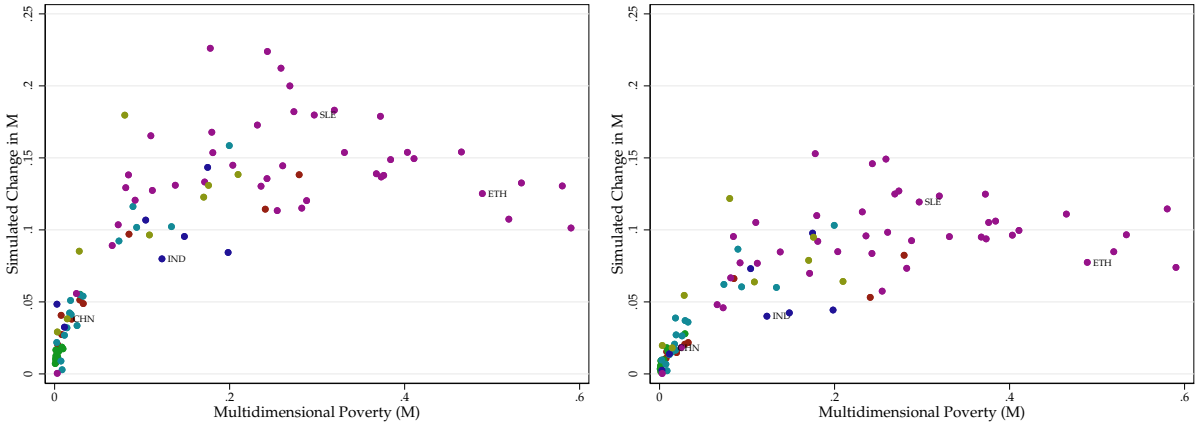

(b) Moderate Impact on Nutrition (25%)

(i) With School Attendance (50%) (ii) Without School Attendance

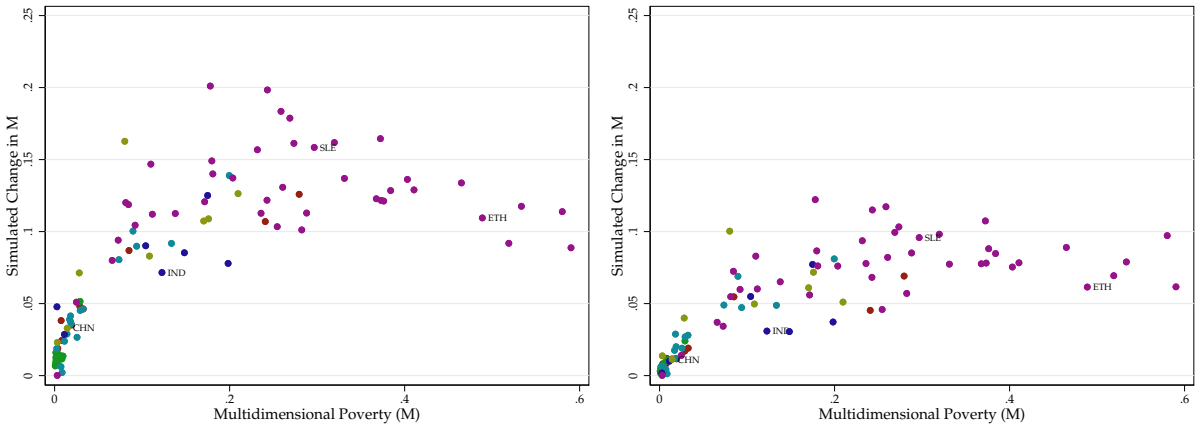

(c) Lower Impact on Nutrition (10%)

(i) With School Attendance (50%) (ii) Without School Attendance

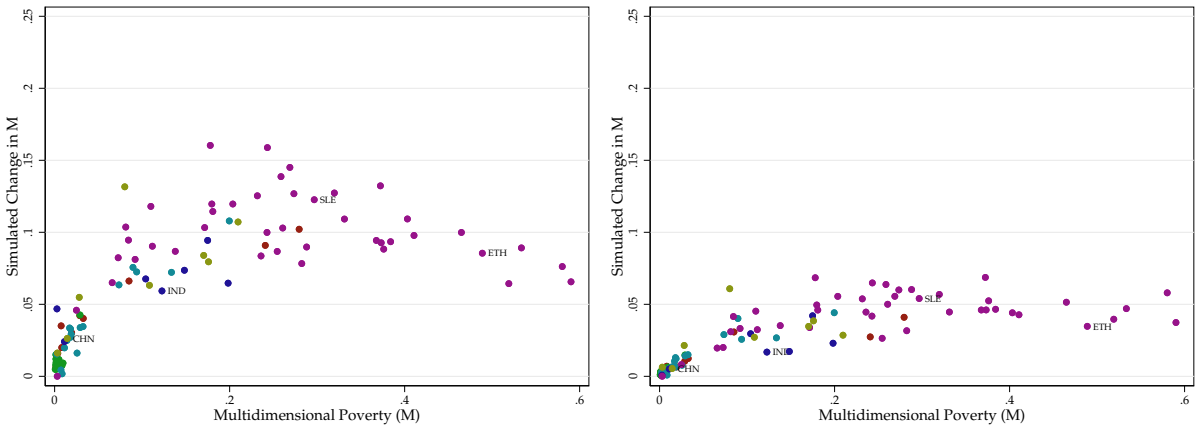

Notes: Simulated increase in multidimensional poverty under microsimulations implementing indicated scenarios. Selected countries labelled: China (CHN), India (IND), Sierra Leone (SLE) and Ethiopia (ETH). Countries are colour-coded by world region: ● Arab States; ● East Asia and the Pacific; ● Europe and Central Asia; ● Latin America and the Caribbean; ● South Asia; ● Sub-Saharan Africa.

Besides the 25% risk scenario, we also explore other risk levels to simulate the shock to nutrition. A lower risk of 10% is motivated by the potential implementation of policy measures throughout 2020 that seek to prevent the rise in food insecurity as well the possibility that COVID-induced deprivations in nutrition might be less associated with other deprivations and thus not focused on the multidimensionally poor or vulnerable. This we consider a lower-impact scenario. Finally, there is also reason to consider a worst-case or upper-impact scenario with 50%-risk of pandemic-induced undernutrition for the vulnerable or already poor (but not undernourished). The WFP estimates only represent a part of the populations of the countries that they analyse; in a worst-case scenario similar impacts may arise for the remainder of their populations as well as the remaining countries that we analyse.

We implement microsimulations of the impact on multidimensional poverty for each of the 97 countries, under each of these scenarios. As the impact on school attendance may be less persistent than the impact on nutrition, we explore the nutrition scenarios also on their own, yielding a total of six scenarios. The simulated impact on multidimensional poverty (M) under all six scenarios is illustrated in Figure 16.

6.2 Modelling COVID-19 Impact in the Context of Changing Poverty

Our microsimulations necessarily model the impact of the COVID-19 pandemic had it taken place at the same time as the surveys. In fact, the pandemic took hold globally in the early months of 2020.

We will need to account for the progress in poverty reduction that countries have made since the time of their surveys, acknowledging not only that baseline poverty levels (and the underlying distribution of deprivations) will have changed in each country, but also that the impact of the pandemic may be different from the result of our simulation, as a result of these changes. From Figure 16, where the relationship between level of poverty and simulated impact of the pandemic is increasing over much of the domain, it is apparent that most countries that have reduced poverty since their survey are likely to experience a smaller impact from the pandemic in 2020 than they would have done at the time of their survey. Conversely, at very high levels of multidimensional poverty the relation between level and simulated impact reverses. This is quite natural, as in the poorest countries where many households are already deprived in the nutrition and

If there had already been an individual in the household who was undernourished, the household would already have been deprived in nutrition and so deprivation according to the indicator definition of the global MPI will not increase.

school attendance indicators, there is less 'space' for the pandemic to increase deprivations. Therefore, some of the poorest countries that have reduced poverty since their survey may actually experience a greater impact from the pandemic in 2020 than they would have done at the time of their survey.

To account for these effects, we start by modelling the relationship between simulated effects of the pandemic and baseline poverty levels across countries. For each scenario we estimate simple parametric models of simulated impacts on multidimensional poverty M and its incidence H, as a function of incidence H and intensity A. There is one observation for each country, whose time-period is the global MPI survey date in each case; time subscripts are dropped to simplify notation.

Table 7: COVID-19 Model Selection for H (Moderate Nutrition (25%) and Education (50%) Scenario)

	(1) $\Delta^* H$	(2) $\Delta^* H$	(3) $\Delta^* H$	(4) $\Delta^* H$	(5) $\Delta^* H$
H	0.125***	0.743***	0.999***	1.550***	1.106***
	(4.94)	(15.68)	(9.02)	(14.58)	(5.54)
H^2		-0.830***	-1.666***		-0.551*
		(-13.72)	(-4.98)		(-2.60)
H^3			0.662*		
			(2.54)		
A				0.432*	-0.141
				(2.24)	(-0.49)
HA				-2.683***	-0.930
				(-13.41)	(-1.33)
Constant	0.0907***	0.0409***	0.0316***	-0.115	0.0954
	(9.07)	(5.97)	(4.17)	(-1.56)	(0.88)
Observations	97	97	97	97	97
Adjusted R^2	0.196	0.729	0.744	0.731	0.747

Notes: Own calculations, t-statistics in parentheses, indicated levels of significance are * $p < 0.05$, ** $p < 0.01$, *** $p < 0.001$. See A.1 for the list of datasets underlying these results.

Table 7 reports results from regressions of $\Delta^* H$, the simulated impact of the pandemic on H, on powers of H and A. The simulated impacts are those obtained under the scenario in which the pandemic has a moderate impact on nutrition (25% of the poor or vulnerable but not undernourished become undernourished) and an impact on education (50% of primary aged children in school stop attending). The quadratic specification in H (model 2) explains 73% of the variation in $\Delta^* H$ across countries, clearly dominating the linear specification (model 1). Adding a cubic term (model 3) or A and its interaction with H (models 4 and 5) increases fit only marginally, so we select the quadratic model. Similar results are obtained for all six scenarios. The chosen model is thus

$$\Delta^* H_s = \gamma_0 + \gamma_1 H_s + \gamma_2 H_s^2 + u_s. \tag{11}$$

Given least squares estimates $\hat{\gamma}_0$, $\hat{\gamma}_1$ and $\hat{\gamma}_2$, the residual for country s is

$$\hat{u}_s = \Delta^* H_s - \hat{\gamma}_0 - \hat{\gamma}_1 H_s - \hat{\gamma}_2 H_s^2. \tag{12}$$

The Breusch-Pagan test rejects the hypothesis of homoskedasticity ($p = 0.008$ for this scenario).

Table 8: COVID-19 Model Selection for M (Moderate Nutrition (25%) and Education (50%) Scenario)

	(1) $\Delta^* M$	(2) $\Delta^* M$	(3) $\Delta^* M$	(4) $\Delta^* M$	(5) $\Delta^* M$	(6) $\Delta^* M$	(7) $\Delta^* M$	(8) $\Delta^* M$
H	0.156***	0.458***	0.896***	0.808***	0.899***			
	(11.98)	(17.42)	(16.51)	(7.71)	(16.54)			
H^2		-0.406***		-0.108				
		(-12.09)		(-0.97)				
A			0.124	0.0122				
			(1.27)	(0.08)				
HA			-1.348***	-1.004**	-1.296***			
			(-13.21)	(-2.72)	(-13.80)			
M						0.242***	0.778***	1.143***
						(9.47)	(17.09)	(11.92)
M^2							-1.178***	-3.166***
							(-12.54)	(-6.64)
M^3								2.526***
								(4.24)
Const.	0.0386***	0.0142***	-0.0299	0.0113	0.0176***	0.0475***	0.0220***	0.0144***
	(7.54)	(3.75)	(-0.79)	(0.20)	(5.31)	(8.64)	(5.58)	(3.55)
Obs.	97	97	97	97	97	97	97	97
Adj. R^2	0.598	0.841	0.866	0.866	0.866	0.480	0.804	0.834

Notes: Own calculations, t-statistics in parentheses, indicated levels of significance are * $p < 0.05$, ** $p < 0.01$, *** $p < 0.001$. See A.1 for the list of datasets underlying these results.

Table 8 reports results from regressions of $\Delta^* M$, the simulated impact of the pandemic on M, on powers of H, A and M. The simulated impacts are again those obtained under the scenario in which the pandemic has a moderate impact on nutrition (25% of the poor or vulnerable but not undernourished become undernourished) and an impact on education (50% of primary aged children in school stop attending). The quadratic specification in H (model 2) explains 84% of the variation in $\Delta^* M$ across countries, again dominating the linear specification (model 1). Replacing H^2 with A and its interaction with H (model 3) increases fit to 87%, not changed by addition of H^2 (model 4) or dropping A (model 5), whose coefficient was insignificant in model 3.

We may ask whether modelling $\Delta^* M$ as a function of M itself performs any better than as a function of H and A. Models (3–5) explain more of the variation in $\Delta^* M$ than polynomial functions of M (models 6–8), so we choose model 5 as our preferred model

for the simulated impact of the pandemic $\Delta^* M$. Similar results are obtained for all six scenarios. The chosen model is thus

$$\Delta^* M_s = \eta_0 + \eta_1 H_s + \eta_2 H_s A_s + v_s. \tag{13}$$

Given least squares estimates $\hat{\eta}_0$, $\hat{\eta}_1$ and $\hat{\eta}_2$, the residual for country s is

$$\hat{v}_s = \Delta^* M_s - \hat{\eta_0} - \hat{\eta_1} H_s - \hat{\eta_2} H_s A_s. \tag{14}$$

The Breusch-Pagan test rejects the hypothesis of homoskedasticity ($p = 0.001$ for this scenario).

We recognise that country-specific factors are fundamentally important in modelling the impact of the pandemic: the existing joint distribution of global MPI indicators varies across countries, making poverty in some countries more sensitive than in others to the simulated scenarios. This is apparent in Tables 7 and 8; our preferred models, despite achieving high explanatory power, do not explain all of the variation in simulated impacts across countries. It is also apparent in Figure 16, which illustrates moderate variation in simulated impacts conditional on the baseline level of poverty.

It would, therefore, be naive to implement predictions from (11) and (13) without adjusting for country-specific effects. That is, to predict the impact of the pandemic on incidence of multidimensional poverty H for country s in 2020 as

$$\hat{\Delta^* H_s}(2020) = \hat{\gamma_0} + \hat{\gamma_1} \check{H}_s^{\log}(2020) + \hat{\gamma_2} \left(\check{H}_s^{\log}(2020) \right)^2.$$

Implementing this model, a prediction at the time of the country's survey would not coincide with the simulated impact.

This could be corrected by adding the country-specific residual (12), so that

$$\hat{\Delta^* H_s}(2020) = \hat{\gamma_0} + \hat{\gamma_1} \check{H}_s^{\log}(2020) + \hat{\gamma_2} \left(\check{H}_s^{\log}(2020) \right)^2 + \hat{u}_s.$$

However, this approach allows predicted impacts to be negative, which is not possible in the scenarios implemented, and does not respect the heteroskedasticity observed. Rather than making additive country-specific adjustments, we therefore make multiplicative adjustments, computing country-specific adjustment factors

$$\hat{\phi}_s = \frac{\Delta^* H_s}{\hat{\gamma_0} + \hat{\gamma_1} H_s + \hat{\gamma_2} H_s^2}$$

so that

$$\hat{\Delta^* H_s}(2020) = \hat{\phi}_s \left(\hat{\gamma_0} + \hat{\gamma_1} \check{H}_s^{\log}(2020) + \hat{\gamma_2} \left(\check{H}_s^{\log}(2020) \right)^2 \right). \tag{15}$$

Figure 17: Country-Specific Models of Simulated Impact of COVID-19 on Incidence of Multidimensional Poverty

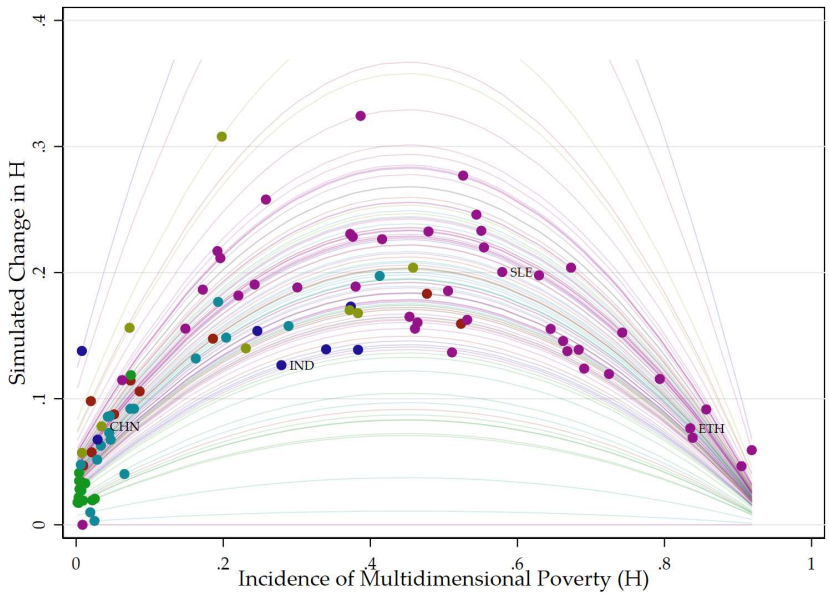

Notes: Simulated increase in multidimensional poverty incidence (H) under microsimulations implementing the moderate nutrition (25%) and school attendance (50%) scenario. Selected countries labelled: China (CHN), India (IND), Sierra Leone (SLE) and Ethiopia (ETH). Countries are colour-coded by world region: ● Arab States; ● East Asia and the Pacific; ● Europe and Central Asia; ● Latin America and the Caribbean; ● South Asia; ● Sub-Saharan Africa. Lines represent country-specific models.

Equation (15) is our country- and scenario-specific model for the impact of the pandemic on the incidence of multidimensional poverty. Figure 17 illustrates such models for the scenario in which the pandemic causes a moderate impact on nutrition (25% of the poor or vulnerable but not undernourished become undernourished) and and impact on school attendance (50% of primary age children in school stop attending).

Similarly, for M we compute adjustment factors

$$\hat{\psi}_s = \frac{\Delta^* M_s}{\hat{\eta}_0 + \hat{\eta}_1 H_s + \hat{\eta}_2 H_s A_s}.$$

giving our country- and scenario-specific model for the impact of the pandemic on the level of multidimensional poverty

$$\Delta^* \hat{M}_s(2020) = \hat{\psi}_s \left(\hat{\eta}_0 + \hat{\eta}_1 \check{H}_s^{\log}(2020) + \hat{\eta}_2 \check{H}_s^{\log}(2020) \check{A}_s^{\mathrm{ml}}(2020) \right). \tag{16}$$

Figure 18 illustrates such models for the scenario in which the pandemic causes a moderate impact on nutrition (25% of the poor or vulnerable but not undernourished become undernourished) and and impact on school attendance (50% of primary age children in school stop attending).

Figure 18: Country-Specific Models of Simulated Impact of COVID-19 on Multidimensional Poverty

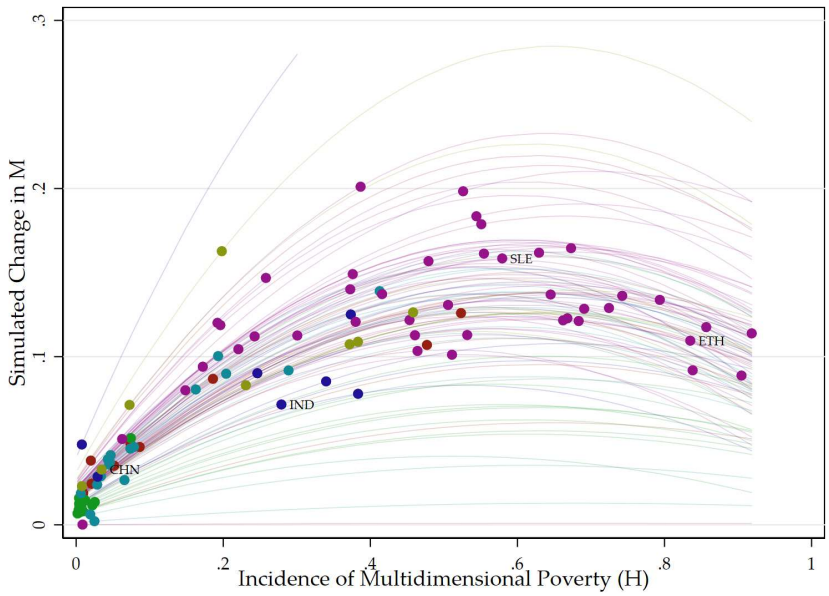

Notes: Simulated increase in multidimensional poverty (M) under microsimulations implementing the moderate nutrition (25%) and school attendance (50%) scenario. Selected countries labelled: China (CHN), India (IND), Sierra Leone (SLE) and Ethiopia (ETH). Countries are colour-coded by world region: ● Arab States; ● East Asia and the Pacific; ● Europe and Central Asia; ● Latin America and the Caribbean; ● South Asia; ● Sub-Saharan Africa. Lines represent country-specific models.

6.3 Impact on Global Poverty Projections

We now combine the results of the microsimulations with our preferred logistic model projection results from section 5, to model the impact of the COVID-19 pandemic on global poverty in 2020. Throughout this section we restrict attention to those 70 countries that include the nutrition indicator and for which we have projection results (see Table A.1 for a list).

Our assessment of the impact of the pandemic on global poverty follows several steps.

(1) For each country, we:

   (a) Calibrate the logistic projection models using the Changes over Time data as described in section 4.4 and apply the calibrated β parameters to project the global MPI forward to 2020.

   (b) Simulate the impact if the pandemic had taken place concurrently with the survey, as described in section 6.1.

   (c) Apply the country-, index- and simulation-specific COVID-19 impact model described in section 6.2 to model the impact of the pandemic, given that it takes place in 2020.

(2) For all 70 countries analysed, we then:

   (a) Aggregate the projected global MPI (M) trajectories (weighting by UN-DESA medium-fertility population projections for each year).

   (b) Aggregate the simulation-specific COVID-19 impacts on M to determine the aggregate increase in multidimensional poverty across the 70 countries, again population-weighted.

   (c) Compare the resulting level of aggregate multidimensional poverty (M) to its aggregate trajectory, to determine the number of years that the pandemic would set back poverty reduction across the 70 countries under the scenario implemented.

(3) For all 70 countries analysed, we also:

   (a) Combine the simulation-specific COVID-19 impact on H with the UN-DESA medium-fertility population projection for 2020 to determine the potential increase in the number of people in multidimensional poverty in that scenario.

   (b) Aggregate the increases in number of people in multidimensional poverty to determine the total number of people pushed into poverty in that scenario, across the 70 countries.

Our aggregate results for each of the scenarios are summarised in Table 9 and illustrated in Figure 19. Pre-COVID-19 projections are 0.095 for MPI value and 941 million for the number of people in multidimensional poverty across the 70 countries in 2020. We find that the COVID-19 pandemic threatens to considerably aggravate this situation, erasing significant progress achieved in poverty reduction. The impact in the scenarios with combined nutrition and school attendance shocks is large. The MPI value rises up to 0.164 in the 50%-nutrition and 50% school attendance (upper-limit) simulation, which implies 547 million more people living in multidimensional poverty. This situation corresponds to a 9.9-year setback to achieved progress in poverty reduction. Even in the scenarios that consider solely nutrition shocks, the MPI value could rise up to 0.134 (50%-nutrition), with 310 million more people in poverty. This corresponds to a 6.4-year setback in the poverty reduction process. Even in our most conservative scenario, the low-impact scenario in which 10% of the poor and vulnerable but not undernourished become undernourished, with no persistent impact on school attendance, we find that 131 million more people would be poor (with an MPI value of 0.112) setting us back 3.1 years.

Table 9: Summary of COVID-19 Simulation Results

COVID-19 scenario		Projection for 2020		
Selection probabilities				
Nutrition	School attendance	MPI	Δ # poor	Setback
(%)		value	(million)	(years)
10	–	0.112	131	3.1
25	–	0.125	237	5.2
50	–	0.134	310	6.4
10	50	0.144	413	7.8
20	50	0.156	490	9.1
50	50	0.164	547	9.9

Notes: Authors' calculations. For a detailed description of the underlying scenarios see section section 6.1.

Figure 19: Impact of COVID-19 on Multidimensional Poverty

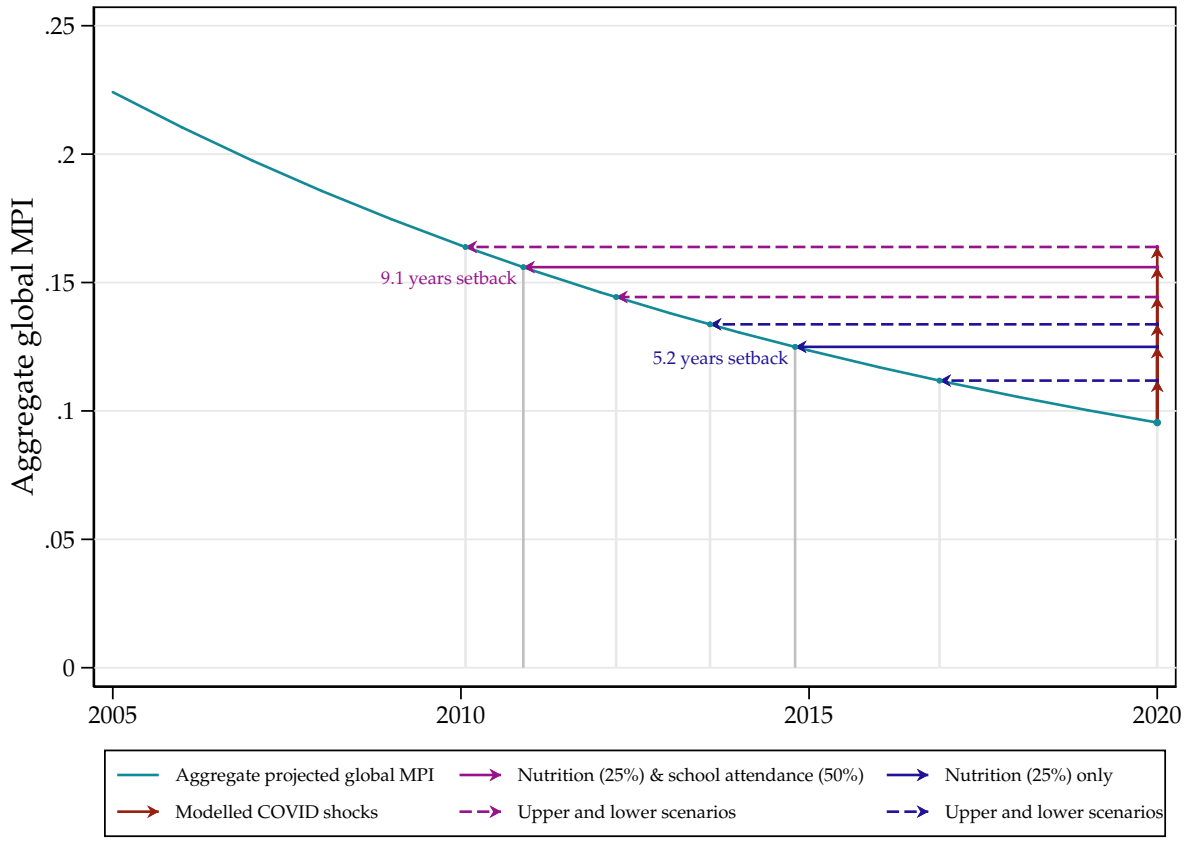

Notes: For a detailed description of the underlying scenarios see section 6.1.

6.3.1 Data Complexities

In most cases (59 of the 70 countries) the global MPI micro data source is the same as that used for the t_2 harmonised estimates in the Changes over Time dataset; however, for

11 countries the global MPI micro data is more recent.[13] Furthermore, the harmonisation process resulted in some minor discrepancies between global MPI and Changes over Time estimates of multidimensional poverty.[14]

Our modelling approach allows for discrepancies in timing and estimates by applying the β parameters obtained from calibration of the projection models with the Changes over Time data while adjusting the α parameters where necessary to align with the global MPI estimates. In the case of timing discrepancies, the implicit assumption is that β is stable over time. As the calibrated β parameters vary remarkably little across countries at different stages of the development process (see section 4.4), we are relaxed about this assumption. Similarly, the harmonised estimates of multidimensional poverty differ very little from the global MPI estimates, so we would not expect there to be any significant differences in the β parameters, were it possible to calibrate them for the global MPI estimates.[15]

7 Concluding Remarks

In this paper, we present projections of multidimensional poverty for 75 countries. Furthermore, to explore the impact of COVID-19 on multidimensional poverty levels globally, we evaluate plausible setbacks to progress in poverty reduction induced by simulated deprivations in nutrition and school attendance. The value-added of this paper is two-fold. On the one hand it proposes methodological advancements to identify multidimensional poverty time-paths, and on the other hand it offers novel empirical results that are useful for policy purposes. Throughout the paper we focus on the most widely known approach to multidimensional poverty measurement—namely the global MPI and its subindices.

This paper develops and calibrates models for multidimensional poverty trajectories drawing on two periods of data for 75 countries in the developing world. Our analytical approach allows us to accommodate current data limitations while exploring, theoretically and empirically, alternative canonical models for these trajectories: linear, constant relative change and logistic. Among these three options, we make a strong case for logistic models as the most appropriate for the subindices of multidimensional poverty, both because they respect the double-bounded nature of these indices and because their theoretical characteristics are strongly supported by our cross-country data. On these solid

[13] These 11 countries are Democratic Republic of the Congo, Gambia, Guinea, Kyrgyzstan, Lesotho, Mali, Mongolia, Suriname, Togo, Zambia and Zimbabwe.

[14] These discrepancies are very small; the correlation between estimates of H in the global MPI and Changes over Time data is 0.999 across the 59 countries for which the same data source is used, and 0.998 for M.

[15] This is not possible, because we need at least two observations at different points in time to calibrate the β parameters.

grounds, we were able to calibrate a set of country-specific trajectories of multidimensional poverty, yielding projections of yearly poverty levels from 2000 to 2030 for all 75 considered countries.

Our empirical results rely on a unique, strictly harmonized dataset of multidimensional poverty changes over time, which we used to calibrate all three models for each country (linear, constant relative change and logistic). This allowed us to perform an empirical assessment of progress made so far in terms of poverty reduction that is closely related to SDG 1, target 1.2: we make the first comprehensive evaluation of whether countries would be on track to halve multidimensional poverty between 2015 and 2030 if observed trends continue. Our country-specific calibrated trajectories allowed us to a) project the level of poverty as measured by the MPI, then b) establish the country-specific target of halving multidimensional poverty, and c) compare the latter with the projected poverty level in 2030. For 47 countries, all three models agree that if the observed trends continue, the country will be 'on track' to halving multidimensional poverty, while for 18 countries, all three models agree that they will be 'off track' to meet this target. For ten countries, the results are model-dependent. If the trajectory were to be assessed by the *simple* headcount ratio (incidence) rather than the full measure of multidimensional poverty (the value of the MPI), 43 countries would be on track and the same 18 would be off track.

Recognising that trajectories may accelerate or decelerate, we stress-tested these findings by establishing the stability of these projection results under counterfactual trajectories. Projections based on the logistic model indicate that 22 countries will off track to meet the target if observed trends continue—this agrees with the other two models for 18 countries, and it is model-specific for an additional 4. If we define the 'median' performance in terms of poverty reduction as a trajectory with the observed median annual rate of poverty reduction adjusted by poverty level, then of these 22 countries, 15 will halve MPI if their poverty reduction performance is boosted up to that level. Nevertheless, 7 African countries, some of the poorest ones, will remain off track. Conversely, 11 countries that are on track could falter if their speed of reduction diminished, but what is somewhat heartening is the stability of the positive trajectories even in the face of moderate deceleration of progress.

However, the projections are based on trajectories that obtained prior to the COVID-19 pandemic and accompanying economic upheaval. In the present context, it is essential to adjust expectations of progress given the difficult human tragedies that worryingly loom ahead. A particularly complicated aspect is that poverty measures and trends refer to the living conditions of survivors. High rates of fatality among the poor do not increase measured poverty except insofar as they impact the child mortality indicator of the global MPI, or leave the survivors worse off. Our simulations of the impact of

COVID-19, therefore, simulate the potential increase in deprivations among survivors, using scenarios that reflect predictions of international agencies. Using the underlying 2020 global MPI, the most recent source to compute internationally comparably measures of multidimensional poverty, increases in undernutrition (10%, 25%, and 50% of the poor and vulnerable but not undernourished) are simulated, as are increases in out of school primary children (50% of those in school) across the entire distribution. The increases in poverty levels as measured by the MPI are then adjusted to account for progress to 2020, showing that the COVID-19 shock is likely to set back global multidimensional poverty reduction by at least 3.1 years, and up to 9.9 years.

This paper represents a step forward to a fully-fledged analysis of multidimensional poverty trends. It manages to accommodate important current data limitations using a sound analytical parametric approach. As more data becomes available, it will be possible to introduce complementary statistical approaches, including non-parametric techniques. It may also become possible to assess the role played by covariates of multidimensional poverty in predicting its trends and levels. When it comes to assessing the impact of the COVID-19 pandemic, its fast evolving nature and inherent country context-dependence must be taken into account. Yet any well-informed and methodologically grounded assessment of its possible effects, albeit partial, sheds useful light, to ignite debates and hopefully trigger policy action to prevent (more) damage to human lives and to progress made so far towards ending poverty in all its forms.

In his last book, Measuring Poverty Around the World, Atkinson aimed to "provide the evidence about the extent and nature of poverty that is necessary to spur action and to design effective policies" (Atkinson, 2019). Recognising that exercises related to global poverty may be highly controversial, and flawed, but nonetheless useful, this paper has sought to complement efforts to improve the measurement of global poverty, by a new combination of techniques to project multidimensional poverty trajectories and simulate shocks. Given the relevance and level of complexity, this paper is a first rather than a last word on the subject. The aim, through critical exchange, is to strengthen the methods available in ways that might spur both discussion and action.

References

Alkema, L. and New, J.R., 2014. Global estimation of child mortality using a Bayesian B-spline bias-reduction model, *The Annals of Applied Statistics*, 2122–2149.

Alkire, S. and Foster, J., 2011. Counting and multidimensional poverty measurement, *Journal of Public Economics*, 95 (7-8), 476–487.

Alkire, S., Foster, J., Seth, S., Santos, M., Roche, J., and Ballón, P., 2015. *Multidimensional Poverty Measurement and Analysis: A Counting Approach*, Oxford: Oxford University Press.

Alkire, S. and Kanagaratnam, U., forthcoming. Revisions of the global multidimensional poverty index: Indicator options and their empirical assessment, *Oxford Development Studies*.

Alkire, S., Kanagaratnam, U., Nogales, R., and Suppa, N., 2020a. Revising the global multidimensional poverty index: Empirical insight and robustness, OPHI Research in Progress 56a, Oxford Poverty and Human Development Initiative, University of Oxford.

Alkire, S., Kanagaratnam, U., and Suppa, N., 2020b. Global multidimensional poverty index 2020, OPHI MPI Methodological Notes 49, Oxford Poverty and Human Development Initiative, University of Oxford, UK.

Alkire, S., Kovesdi, F., Mitchell, C., Pinilla-Roncancio, M., and Scharlin-Pettee, S., 2020c. Changes over time in the global multidimensional poverty index, OPHI MPI Methodological Notes 50, Oxford Poverty and Human Development Initiative, University of Oxford, UK.

Alkire, S., Kovesdi, F., Pinilla-Roncancio, M., and Scharlin-Pettee, S., 2020d. Changes over time in the global multidimensional poverty index and other measures: Towards national poverty reports, OPHI Research in Progress 57a, Oxford Poverty and Human Development Initiative, University of Oxford, UK.

Alkire, S., Oldiges, C., and Kanagaratnam, U., 2018. Multidimensional poverty reduction in india 2005/6–2015/16: Still a long way to go but the poorest are catching up, OPHI Research in Progress Paper 54a, Oxford Poverty and Human Development Initiative, University of Oxford, Oxford, UK.

Alkire, S., Roche, J.M., and Vaz, A., 2017. Changes over time in multidimensional poverty: Methodology and results for 34 countries, *World Development*, 94, 232–249.

Alkire, S. and Santos, M.E., 2014. Measuring acute poverty in the developing world: Robustness and scope of the multidimensional poverty index, *World Development*, 59, 251–274.

Atkinson, A.B., 2019. *Measuring poverty around the world*, Princeton University Press.

Burchi, F., Malerba, D., Montenegro, C.E., and Rippin, N., 2020. Assessing trends in multidimensional poverty during the MDGs, Global Development Institute Working Paper Series 2020-044, The University of Manchester.

Clemens, M., 2004. The long walk to school: International education goals in historical perspective, Working Paper 37, Center for Global Development.

JCME, 2020. Levels and trends in child malnutrition: Key findings of the 2020 edition of the joint child malnutrition estimates., Report, United Nations Children's Fund (UNICEF), World Health Organization, International Bank for Reconstruction and Development/The World Bank., Geneva.

Klasen, S. and Lange, S., 2012. Getting progress right: Measuring progress towards the mdgs against historical trends, Tech. Rep. 87, Courant Research Centre: Poverty, Equity and Growth-Discussion Papers.

Lange, S., 2014. Projections to zero, Tech. rep., Background paper prepared for the Education for All Global Monitoring Report 2013/14.

Meyer, J.W., Ramirez, F.O., and Soysal, Y.N., 1992. World expansion of mass education, 1870-1980, *Sociology of Education*, 65 (2), 128.

Nicolai, S., Hoy, C., Berliner, T., and Aedy, T., 2015. Projecting progress: reaching the sdgs by 2030, Tech. rep., Overseas Development Institute, London.

Ram, R., 2020. Attainment of multidimensional poverty target of sustainable development goals: a preliminary study, *Applied Economics Letters*, 1–5.

Ravallion, M., 2013. How long will it take to lift one billion people out of poverty?, *The World Bank Research Observer*, 28 (2), 139–158.

Roberton, T., Carter, E.D., Chou, V.B., Stegmuller, A.R., Jackson, B.D., Tam, Y., Sawadogo-Lewis, T., and Walker, N., 2020. Early estimates of the indirect effects of the COVID-19 pandemic on maternal and child mortality in low-income and middle-income countries: a modelling study, *The Lancet Global Health*, 8 (7), e901–e908.

Santos, M.E., Dabus, C., and Delbianco, F., 2019. Growth and poverty revisited from a multidimensional perspective, *The Journal of Development Studies*, 55 (2), 260–277.

UN IGME, 2019. Levels and trends in child mortality 2019, Report, United Nations Interagency Group for Child Mortality Estimation, New York.

UNDP, OPHI, 2020. *Global MPI 2020 — Charting pathways out of multidimensional poverty: Achieving the SDGs*, UNDP.

UNESCO, 2020. Tracking covid-19 caused school and university closures, Methodological Note, 20 April 2020.

WFP, 2020. Global report on food crises: Joint analysis for better decisions., Rome.

WHO-UNICEF, 2017. Methodology for monitoring progress towards the global nutrition targets for 2025, Report, World Health Organization and the United Nations Children's Fund (UNICEF) Technical Expert Advisory Group on Nutrition Monitoring (TEAM).

World Bank, 2017. *Monitoring Global Poverty: Global Report of the Commission on Global Poverty*, World Bank Publications.

World Bank, 2018. Poverty and shared prosperity 2018: Piecing together the poverty puzzle, Report, World Bank, Washington, DC.

A Datasets and Additional Results

Table A.1: Survey datasets

		Changes over Time t_1		Changes over Time t_2		Global MPI		Analysis	
Code	Name	Survey	Year	Survey	Year	Survey	Year	Projection	Simulation
AFG	Afghanistan	MICS	2010/11	DHS	2015/16	DHS	2015/16		
AGO	Angola					DHS	2015/16		•
ALB	Albania	DHS	2008/09	DHS	2017/18	DHS	2017/18	•	•
ARM	Armenia	DHS	2010	DHS	2015/16	DHS	2015/16	•	•
BDI	Burundi	DHS	2010	DHS	2016/17	DHS	2016/17	•	•
BEN	Benin	MICS	2014	DHS	2017/18	DHS	2017/18	•	•
BFA	Burkina Faso	MICS	2006	DHS	2010	DHS	2010	•	•
BGD	Bangladesh	DHS	2014	MICS	2019	MICS	2019	•	•
BIH	Bosnia and Herzegovina	MICS	2006	MICS	2011/12	MICS	2011/12	•	•
BLZ	Belize	MICS	2011	MICS	2015/16	MICS	2015/16	•	•
BOL	Bolivia	DHS	2003	DHS	2008	DHS	2008	•	•
BRA	Brazil					PNAD	2015		
BRB	Barbados					MICS	2012		•
BTN	Bhutan					MICS	2010		•
BWA	Botswana					BMTHS	2015/16		•
CAF	Central African Republic	MICS	2000	MICS	2010	MICS	2010	•	•
CHN	China	CFPS	2010	CFPS	2014	CFPS	2014	•	•
CIV	Côte d'Ivoire	DHS	2011/12	MICS	2016	MICS	2016	•	•
CMR	Cameroon	DHS	2011	MICS	2014	MICS	2014	•	•
COD	Congo, DR	DHS	2007	DHS	2013/14	MICS	2017/18	•	•
COG	Congo	DHS	2005	MICS	2014/15	MICS	2014/15	•	•
COL	Colombia	DHS	2010	DHS	2015	DHS	2015/16	•	
COM	Comoros					DHS	2012		•
CUB	Cuba					ENO	2017		
DOM	Dominican Republic	DHS	2007	MICS	2014	MICS	2014	•	
DZA	Algeria					MICS	2012/13		•
ECU	Ecuador					ECV	2013/14		•
EGY	Egypt	DHS	2008	DHS	2014	DHS	2014	•	•
ETH	Ethiopia	DHS	2011	DHS	2016	DHS	2016	•	•
GAB	Gabon	DHS	2000	DHS	2012	DHS	2012	•	•
GEO	Georgia					MICS	2018		•
GHA	Ghana	MICS	2011	DHS	2014	DHS	2014	•	•
GIN	Guinea	DHS	2012	MICS	2016	DHS	2018	•	•
GMB	Gambia	MICS	2005/06	DHS	2013	MICS	2018	•	•
GNB	Guinea-Bissau					MICS	2014		•
GTM	Guatemala					DHS	2014/15		•
GUY	Guyana	DHS	2009	MICS	2014	MICS	2014	•	•
HND	Honduras	DHS	2005/06	DHS	2011/12	DHS	2011/12	•	•
HTI	Haiti	DHS	2012	DHS	2016/17	DHS	2016/17	•	•
IDN	Indonesia	DHS	2012	DHS	2017	DHS	2017	•	
IND	India	DHS	2005/06	DHS	2015/16	DHS	2015/16	•	•
IRQ	Iraq	MICS	2011	MICS	2018	MICS	2018	•	•
JAM	Jamaica	JSLC	2010	JSLC	2014	JSLC	2014	•	•
JOR	Jordan	DHS	2012	DHS	2017/18	DHS	2017/18	•	•
KAZ	Kazakhstan	MICS	2010/11	MICS	2015	MICS	2015	•	•
KEN	Kenya	DHS	2008/09	DHS	2014	DHS	2014	•	•
KGZ	Kyrgyzstan	MICS	2005/06	MICS	2014	MICS	2018	•	•
KHM	Cambodia	DHS	2010	DHS	2014	DHS	2014	•	•
KIR	Kiribati					MICS	2018/19		•
LAO	Lao PDR	MICS-DHS	2011/12	MICS	2017	MICS	2017	•	•
LBR	Liberia	DHS	2007	DHS	2013	DHS	2013	•	•
LBY	Libya					PAPFAM	2014		•
LCA	Saint Lucia					MICS	2012		•
LKA	Sri Lanka					SLDHS	2016		•
LSO	Lesotho	DHS	2009	DHS	2014	MICS	2018	•	•

... Table A.1 continued.

		Changes over Time t_1		Changes over Time t_2		Global MPI		Analysis	
Code	Name	Survey	Year	Survey	Year	Survey	Year	Projection	Simulation
MAR	Morocco					PAPFAM	2011		•
MDA	Moldova	DHS	2005	MICS	2012	MICS	2012	•	•
MDG	Madagascar	DHS	2008/09	MICS	2018	MICS	2018	•	•
MDV	Maldives					DHS	2016/17		•
MEX	Mexico	ENSANUT	2012	ENSANUT	2016	ENSANUT	2016	•	•
MKD	North Macedonia	MICS	2005/06	MICS	2011	MICS	2011	•	•
MLI	Mali	DHS	2006	MICS	2015	DHS	2018	•	•
MMR	Myanmar					DHS	2015/16		•
MNE	Montenegro	MICS	2005/06	MICS	2013	MICS	2018		•
MNG	Mongolia	MICS	2010	MICS	2013	MICS	2018	•	•
MOZ	Mozambique	DHS	2003	DHS	2011	DHS	2011	•	•
MRT	Mauritania	MICS	2011	MICS	2015	MICS	2015	•	•
MWI	Malawi	DHS	2010	DHS	2015/16	DHS	2015/16	•	•
NAM	Namibia	DHS	2006/07	DHS	2013	DHS	2013	•	•
NER	Niger	DHS	2006	DHS	2012	DHS	2012	•	•
NGA	Nigeria	DHS	2013	DHS	2018	DHS	2018	•	•
NIC	Nicaragua	DHS	2001	ENDESA	2011/12	DHS	2011/12	•	•
NPL	Nepal	DHS	2011	DHS	2016	DHS	2016	•	•
PAK	Pakistan	DHS	2012/13	DHS	2017/18	DHS	2017/18	•	•
PER	Peru	DHS-Cont	2012	DHS	2018	ENDES	2018	•	•
PHL	Philippines	DHS	2013	DHS	2017	DHS	2017	•	
PNG	Papua New Guinea					DHS	2016/18		
PRY	Paraguay					MICS	2016		•
PSE	Palestine, State of	MICS	2010	MICS	2014	MICS	2014	•	•
RWA	Rwanda	DHS	2010	DHS	2014/15	DHS	2014/15	•	•
SDN	Sudan	MICS	2010	MICS	2014	MICS	2014	•	•
SEN	Senegal	DHS	2005	DHS-Cont	2017	DHS	2017	•	•
SLE	Sierra Leone	DHS	2013	MICS	2017	MICS	2017	•	•
SLV	El Salvador					MICS	2014		•
SRB	Serbia	MICS	2010	MICS	2014	MICS	2014	•	•
SSD	South Sudan					MICS	2010		•
STP	Sao Tome and Principe	DHS	2008/09	MICS	2014	MICS	2014	•	•
SUR	Suriname	MICS	2006	MICS	2010	MICS	2018	•	•
SWZ	eSwatini	MICS	2010	MICS	2014	MICS	2014	•	•
SYC	Seychelles					QLFS	2019		•
SYR	Syria					PAPFAM	2009		•
TCD	Chad	MICS	2010	DHS	2014/15	DHS	2014/15	•	•
TGO	Togo	MICS	2010	DHS	2013/14	MICS	2017	•	•
THA	Thailand	MICS	2012	MICS	2015/16	MICS	2015/16	•	•
TJK	Tajikistan	DHS	2012	DHS	2017	DHS	2017	•	•
TKM	Turkmenistan	MICS	2006	MICS	2015/16	MICS	2015/16	•	•
TLS	Timor-Leste	DHS	2009/10	DHS	2016	DHS	2016	•	•
TTO	Trinidad and Tobago	MICS	2006	MICS	2011	MICS	2011		•
TUN	Tunisia					MICS	2018		•
TZA	Tanzania	DHS	2010	DHS	2015/16	DHS	2015/16	•	•
UGA	Uganda	DHS	2011	DHS	2016	DHS	2016	•	•
UKR	Ukraine	DHS	2007	MICS	2012	MICS	2012	•	
VNM	Vietnam	MICS	2010/11	MICS	2014	MICS	2013/14		
YEM	Yemen	MICS	2006	DHS	2013	DHS	2013		•
ZAF	South Africa					DHS	2016		•
ZMB	Zambia	DHS	2007	DHS	2013/14	DHS	2018	•	•
ZWE	Zimbabwe	DHS	2010/11	DHS	2015	MICS	2019	•	•

Notes: *Projection* indicates countries analysed in section 5, *Simulation* indicates those countries for which COVID-19 impacts were simulated and analysed in sections in sections 6.1 and 6.2. The global setback analysis is based on (sections 6.3) is based on the intersection of both.

Table A.2: Calibrated Parameters, Poverty Targets, and Projections

Country	$\check{\beta}_{hs}^{\log}$	$\check{M}(2015)$	$\check{M}(2030)$	Poverty Target	Outcome	Model Robust
ALB	0.122	0.004	0.001	0.002	Met	Yes
ARM	0.156	0.001	0.000	0.000	Met	Yes
BDI	0.067	0.422	0.280	0.211	Not met	Yes
BEN	-0.035	0.351	0.417	0.175	Not met	Yes
BFA	0.056	0.531	0.388	0.265	Not met	Yes
BGD	0.128	0.157	0.026	0.079	Met	Yes
BIH	0.111	0.006	0.001	0.003	Met	Yes
BLZ	0.094	0.021	0.005	0.010	Met	Yes
BOL	0.138	0.039	0.005	0.019	Met	Yes
CAF	0.067	0.431	0.270	0.216	Not met	Yes
CHN	0.217	0.014	0.001	0.007	Met	Yes
CIV	0.115	0.252	0.069	0.126	Met	Yes
CMR	0.030	0.238	0.171	0.119	Not met	Yes
COD	0.032	0.376	0.276	0.188	Not met	Yes
COG	0.133	0.108	0.017	0.054	Met	Yes
COL	0.043	0.020	0.011	0.010	Not met	No
DOM	0.106	0.014	0.003	0.007	Met	Yes
EGY	0.088	0.017	0.004	0.008	Met	Yes
ETH	0.081	0.500	0.315	0.250	Not met	Yes
GAB	0.074	0.056	0.019	0.028	Met	Yes
GHA	0.081	0.107	0.031	0.053	Met	Yes
GIN	0.109	0.355	0.108	0.178	Met	Yes
GMB	0.076	0.255	0.105	0.127	Met	No
GUY	0.109	0.012	0.002	0.006	Met	Yes
HND	0.149	0.058	0.006	0.029	Met	Yes
HTI	0.077	0.207	0.087	0.103	Met	Yes
IDN	0.137	0.018	0.002	0.009	Met	Yes
IND	0.115	0.129	0.026	0.064	Met	Yes
IRQ	0.070	0.044	0.015	0.022	Met	Yes
JAM	0.033	0.017	0.010	0.009	Not met	No
JOR	0.035	0.002	0.002	0.001	Not met	Yes
KAZ	0.146	0.002	0.000	0.001	Met	Yes
KEN	0.099	0.167	0.050	0.084	Met	Yes
KGZ	0.127	0.011	0.002	0.006	Met	Yes
KHM	0.108	0.157	0.038	0.079	Met	Yes
LAO	0.148	0.140	0.016	0.070	Met	Yes
LBR	0.153	0.281	0.047	0.140	Met	Yes
LSO	0.114	0.146	0.032	0.073	Met	Yes

... Table A.2 continued.

Country	$\check{\beta}_{hs}^{\log}$	$\check{M}(2015)$	$\check{M}(2030)$	Poverty Target	Outcome	Model Robust
MDA	0.080	0.003	0.001	0.001	Met	Yes
MDG	0.043	0.391	0.291	0.196	Not met	Yes
MEX	0.040	0.026	0.013	0.013	Not met	No
MKD	0.251	0.003	0.000	0.001	Met	Yes
MLI	0.072	0.417	0.254	0.209	Not met	Yes
MNG	0.161	0.043	0.004	0.021	Met	Yes
MOZ	0.098	0.338	0.130	0.169	Met	No
MRT	0.128	0.260	0.051	0.130	Met	Yes
MWI	0.107	0.260	0.081	0.130	Met	Yes
NAM	0.049	0.147	0.077	0.074	Not met	No
NER	0.065	0.555	0.367	0.278	Not met	Yes
NGA	0.039	0.274	0.183	0.137	Not met	Yes
NIC	0.123	0.049	0.007	0.025	Met	Yes
NPL	0.117	0.143	0.028	0.072	Met	Yes
PAK	0.051	0.215	0.125	0.108	Not met	Yes
PER	0.100	0.039	0.009	0.020	Met	Yes
PHL	0.066	0.032	0.011	0.016	Met	Yes
PSE	0.076	0.003	0.001	0.002	Met	Yes
RWA	0.151	0.248	0.041	0.124	Met	Yes
SDN	0.047	0.271	0.158	0.135	Not met	Yes
SEN	0.040	0.299	0.194	0.150	Not met	Yes
SLE	0.179	0.355	0.051	0.178	Met	Yes
SRB	-0.160	0.002	0.017	0.001	Not met	Yes
STP	0.161	0.080	0.008	0.040	Met	Yes
SUR	0.118	0.020	0.003	0.010	Met	Yes
SWZ	0.138	0.072	0.009	0.036	Met	Yes
TCD	0.015	0.576	0.504	0.288	Not met	Yes
TGO	0.025	0.295	0.236	0.148	Not met	Yes
THA	0.141	0.004	0.001	0.002	Met	Yes
TJK	0.110	0.036	0.007	0.018	Met	Yes
TKM	0.125	0.004	0.001	0.002	Met	Yes
TLS	0.147	0.236	0.039	0.118	Met	Yes
TZA	0.083	0.290	0.137	0.145	Met	No
UGA	0.090	0.295	0.119	0.147	Met	No
UKR	0.083	0.001	0.000	0.000	Met	Yes
ZMB	0.073	0.252	0.113	0.126	Met	No
ZWE	0.059	0.147	0.073	0.073	Met	No

Table A.3: Poverty target by model

Country	$\check{M}^{\log}(2015)$	CRC	Linear	Logistic	Model Robust
ALB	0.004	Met	Met	Met	Yes
ARM	0.001	Met	Met	Met	Yes
BDI	0.422	Not met	Not met	Not met	Yes
BEN	0.351	Not met	Not met	Not met	Yes
BFA	0.531	Not met	Not met	Not met	Yes
BGD	0.157	Met	Met	Met	Yes
BIH	0.006	Met	Met	Met	Yes
BLZ	0.021	Met	Met	Met	Yes
BOL	0.039	Met	Met	Met	Yes
CAF	0.431	Not met	Not met	Not met	Yes
CHN	0.014	Met	Met	Met	Yes
CIV	0.252	Met	Met	Met	Yes
CMR	0.238	Not met	Not met	Not met	Yes
COD	0.376	Not met	Not met	Not met	Yes
COG	0.108	Met	Met	Met	Yes
COL	0.020	Not met	Met	Not met	No
DOM	0.014	Met	Met	Met	Yes
EGY	0.017	Met	Met	Met	Yes
ETH	0.500	Not met	Not met	Not met	Yes
GAB	0.056	Met	Met	Met	Yes
GHA	0.107	Met	Met	Met	Yes
GIN	0.355	Met	Met	Met	Yes
GMB	0.255	Not met	Met	Met	No
GUY	0.012	Met	Met	Met	Yes
HND	0.058	Met	Met	Met	Yes
HTI	0.207	Met	Met	Met	Yes
IDN	0.018	Met	Met	Met	Yes
IND	0.129	Met	Met	Met	Yes
IRQ	0.044	Met	Met	Met	Yes
JAM	0.017	Not met	Met	Not met	No
JOR	0.002	Not met	Not met	Not met	Yes
KAZ	0.002	Met	Met	Met	Yes
KEN	0.167	Met	Met	Met	Yes
KGZ	0.011	Met	Met	Met	Yes
KHM	0.157	Met	Met	Met	Yes
LAO	0.140	Met	Met	Met	Yes
LBR	0.281	Met	Met	Met	Yes
LSO	0.146	Met	Met	Met	Yes

... Table A.3 continued.

Country	$\check{M}^{\log}(2015)$	CRC	Linear	Logistic	Model Robust
MDA	0.003	Met	Met	Met	Yes
MDG	0.391	Not met	Not met	Not met	Yes
MEX	0.026	Not met	Met	Not met	No
MKD	0.003	Met	Met	Met	Yes
MLI	0.417	Not met	Not met	Not met	Yes
MNG	0.043	Met	Met	Met	Yes
MOZ	0.338	Not met	Not met	Met	No
MRT	0.260	Met	Met	Met	Yes
MWI	0.260	Met	Met	Met	Yes
NAM	0.147	Not met	Met	Not met	No
NER	0.555	Not met	Not met	Not met	Yes
NGA	0.274	Not met	Not met	Not met	Yes
NIC	0.049	Met	Met	Met	Yes
NPL	0.143	Met	Met	Met	Yes
PAK	0.215	Not met	Not met	Not met	Yes
PER	0.039	Met	Met	Met	Yes
PHL	0.032	Met	Met	Met	Yes
PSE	0.003	Met	Met	Met	Yes
RWA	0.248	Met	Met	Met	Yes
SDN	0.271	Not met	Not met	Not met	Yes
SEN	0.299	Not met	Not met	Not met	Yes
SLE	0.355	Met	Met	Met	Yes
SRB	0.002	Not met	Not met	Not met	Yes
STP	0.080	Met	Met	Met	Yes
SUR	0.020	Met	Met	Met	Yes
SWZ	0.072	Met	Met	Met	Yes
TCD	0.576	Not met	Not met	Not met	Yes
TGO	0.295	Not met	Not met	Not met	Yes
THA	0.004	Met	Met	Met	Yes
TJK	0.036	Met	Met	Met	Yes
TKM	0.004	Met	Met	Met	Yes
TLS	0.236	Met	Met	Met	Yes
TZA	0.290	Not met	Met	Met	No
UGA	0.295	Not met	Met	Met	No
UKR	0.001	Met	Met	Met	Yes
ZMB	0.252	Not met	Met	Met	No
ZWE	0.147	Not met	Met	Met	No

B Simulation scenarios: Background

B.1 Nutrition Scenarios

The WFP projected that 265 million would be food insecure, and that 130 million were newly food insecure WFP (2020). Their estimation was based on 55 countries. The study of trends in MPI over time covers 49 of those countries each of which contain data for nutrition.

Poor or Vulnerable: Our simulations focus on people who are already poor, or are vulnerable thus deprived in 20% or more of the weighted indicators. If they are vulnerable, then having one additional deprivation in nutrition (or school attendance) will mean that they become poor. If they are already poor, their deprivation score will increase. So in either case there is a visible impact on MPI.

Nutritional Deprivations: Using 2018 data, the 49 countries covered are home to about 1.6 billion people of whom nearly 1 billion (995 million) people are MPI poor or vulnerable. Among these, over 500 million persons (502 million) are poor or vulnerable, and live in a household where at least one person is undernourished. So about 493 million people live in a household in which no one is undernourished.

Five Considerations: WFP predicted an increase of food insecurity by 130 million among sampled areas of those countries. How do we draw on this to set our simulation scenarios? There are five difficult considerations, whose implications are various and difficult to quantify:

(1) Different Countries: We only cover 49 of the 55 countries, hence the number of newly food insecure in these countries is lower.

(2) Not Nationally Representative: The figure of 130 million is an underestimate for these countries, because as detailed in Table 3 of FSIN report, only 21 countries were fully sampled; in 34 countries subgroups were sampled. Overall, 55.6% of the population of the covered countries are sampled in the WFP study . Hence the number of newly food insecure in the 34 countries will be higher.

(3) Different Variable: Food insecurity is linked to but not the same as undernutrition. The increase in undernutrition is likely to be higher than the increase in food security, but could be lower

(4) Not all new deprivations change poverty: The MPI will visibly increase when undernutrition strikes households that are not currently deprived. But increases in food insecurity in already poor and nutritionally deprived households do not change MPI.

(5) Not all countries not covered. The WFP countries are overall, slightly poorer than the other countries covered by the global MPI 2020 and even the trend analysis. But in terms of nutrition, the WFP does not cover India that has a high number of undernourished.

In terms of consideration 1, from Table 6 and 9 of Global Report on Food Insecurity, we do not have nutritional data for Afghanistan and Cabo Verde, where predicted food insecurity will rise by 11.3 million. So the predicted number of newly food insecure in our covered areas of 49 countries is 118.7 million.

Medium Scenario: (25%): Here we presume that the considerations 2-5 balance out. That is, we presume that the significantly higher numbers than 130 million that come from other regions in the countries which were not sampled, very roughly balance. That is, the number of food insecure who are not malnourished, broadly translate into new nutritional deprivations among already poor and nutritionally deprived households. If this were the case, then 118.7 million / 490 million is 24.2% which we increment to 25%. That, then, is our medium or base scenario.

Lower Bound (10%): Recognising that the WFP projections were based on household-wide food insecurity, we presume that the density of food insecurity by households will be higher. So we make the assumption that only a subset of the newly food insecure would visibly affect measured poverty in households who are currently poor or deprived, but not deprived in nutrition. The other deprivations would accrue in already poor households. In that case, the increment among poor or vulnerable households would be then 59.4/ 490 million or 12.1%. That might be compatible with a 'low' scenario of 15%, but to be definitively lower bound, our lower bound scenario is fixed at 10%.

Upper Bound (50%): Finally, our upper bound scenario seeks to quantify consideration 2. above, plus add in the school attendance figure. We first describe the nutrition assumption. Recall that the WFP studies covered only 55.6% of the populations of the covered countries. If the deprivation in the measured areas (Table 9 of WFP report) are applied proportionally to the rest of the population, then the number of newly food insecure rises to 350 million – an increment of 220 million. However, the populations included in the 55 countries tend to be the poorer regions. If the number of nutritionally deprived in the countries was incremented by only half as much (110 million), the newly food insecure would number roughly 240 million. If nearly all of these struck households that were poor or vulnerable but not previously deprived in nutrition, and if considerations 3-5 balance out, then the upper bound scenario should how an increase of 50%.

B.2 School Attendance Scenario

Finally, we move to school attendance. In the 107 countries covered, roughly 530 million people are poor/vulnerable and live in household where at least one child is not attending school. Recall that there are a total of 2.18 billion people who are poor or vulnerable, out of the 5.87 billion persons who are included in the global MPI 2020. So 1.65 billion persons live in a households that is poor or vulnerable but not deprived in school attendance. The increase in out of school children will definitely affect three types of households:

(1) Already deprived in school attendance: if additional children leave school

(2) Poor or vulnerable and have a school-aged child, but not formerly deprived in school attendance

(3) Non-poor, Non-vulnerable, have a school-aged child but not previously deprived in school attendance.

UNESCO data suggest that school closures peaked in April 2020, with over 91 percent of the world's learners out of school (UNESCO, 2020). Subsequently, however, this proportion fell gradually to just over 60 percent in July 2020. These learners include pre-primary school, secondary and secondary school, whereas the global MPI only considers children in classes 1-8. Furthermore, UNESCO (which numbers 1.3 billion affected learners) covers all countries whereas the global MPI only covers 107 countries.

There are roughly 609 million primary school students enrolled in the 107 covered countries, according to the UNESCO website, but not all countries have entries and years vary. We know that in some countries with utter lockdown, 100% of children are out of school. So one option would be to assess that 100% of children were not attending school. However recognising that this is probably a transitory situation, and that in some households, home schooling occurs, we create an intermediate scenario. In particular, we presume that 50% of all primary school aged children (by national definitions) who were attending school, cease to attend schooling of any form. It might be that they have repeated lockdowns; it might be that they never return to school after the lock down. Making even this level of child deprivations visible is already devastating, and hopefully will inform actions to prevent its occurrence.